UNIVERSITAT POLITÈCNICA DE CATALUNYA
BARCELONATECH
Escola Superior d'Enginyeries Industrial, Aeroespacial i Audiovisual de Terrassa

---

Institution

Escola Superior d'Enginyeries Industrial, Aeroespacial i Audiovisual de Terrassa

Degree

Bachelor's degree in Aerospace Vehicle Engineering

Student

Armen Baghdasaryan

Director

Luis Manuel Pérez Llera

Title of the Project

Design of an Unmanned Aerial Vehicle with a Mass-Actuated Control System

---

REPORT ATTACHMENT

Call: Autumn 2019 (Extraordinary)

Date: September 29

Introduction

The aim of this attachment is to provide complementary results and resources achieved during the project development, including plots, tables, scripts and calculations.

Contents

List of Figures

List of Tables

Part A

AERODYNAMICS

Introduction

The aim of this chapter is to provide additional plots and figures obtained from simulations done with XFLR5 and Ansys CFD software.

XFLR5 Design and Simulation

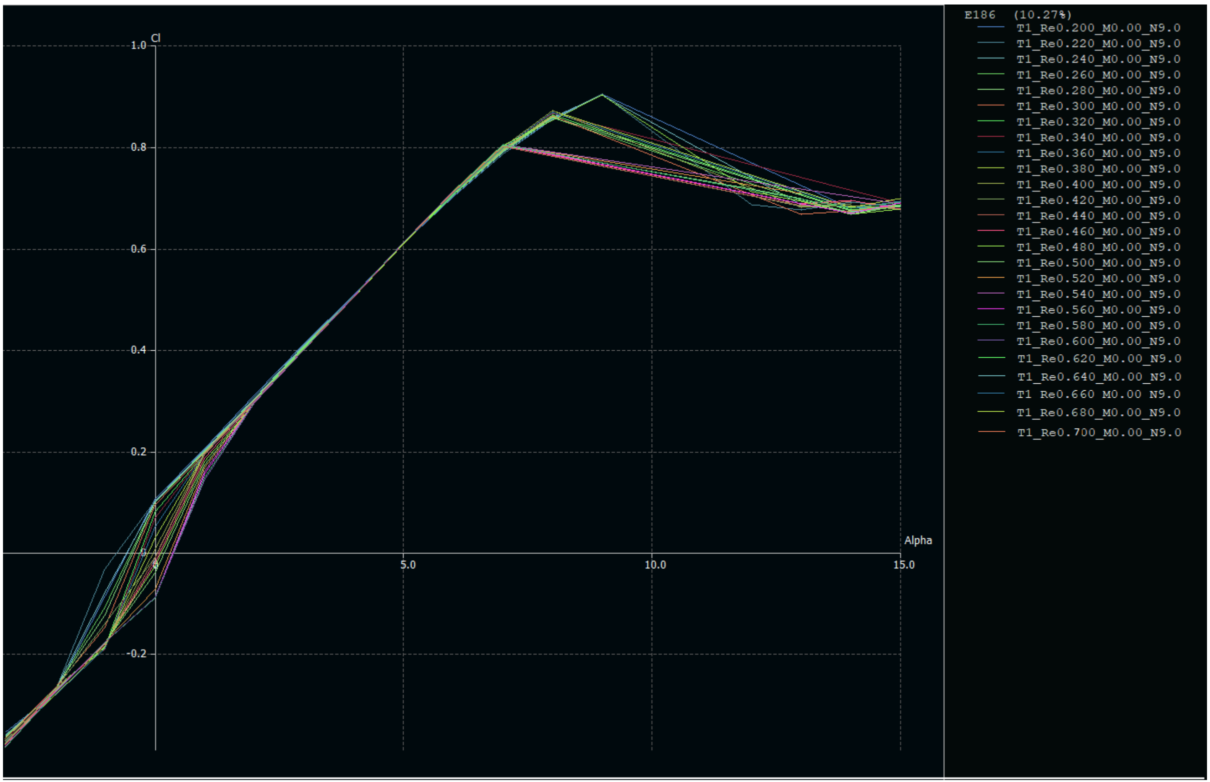

Figure A.1.: Eppler186 Cl – Alpha graph for different Reynolds values, obtained from XFLR5

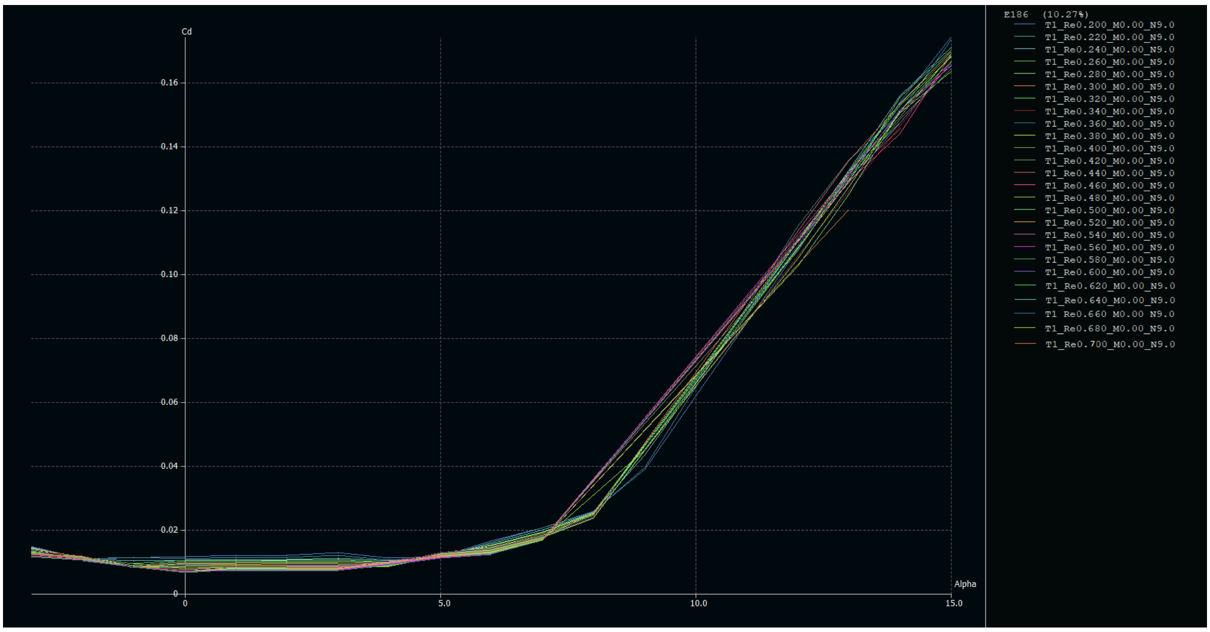

Figure A.2.: Eppler186 Cd – Alpha graph for different Reynolds values, obtained from XFLR5

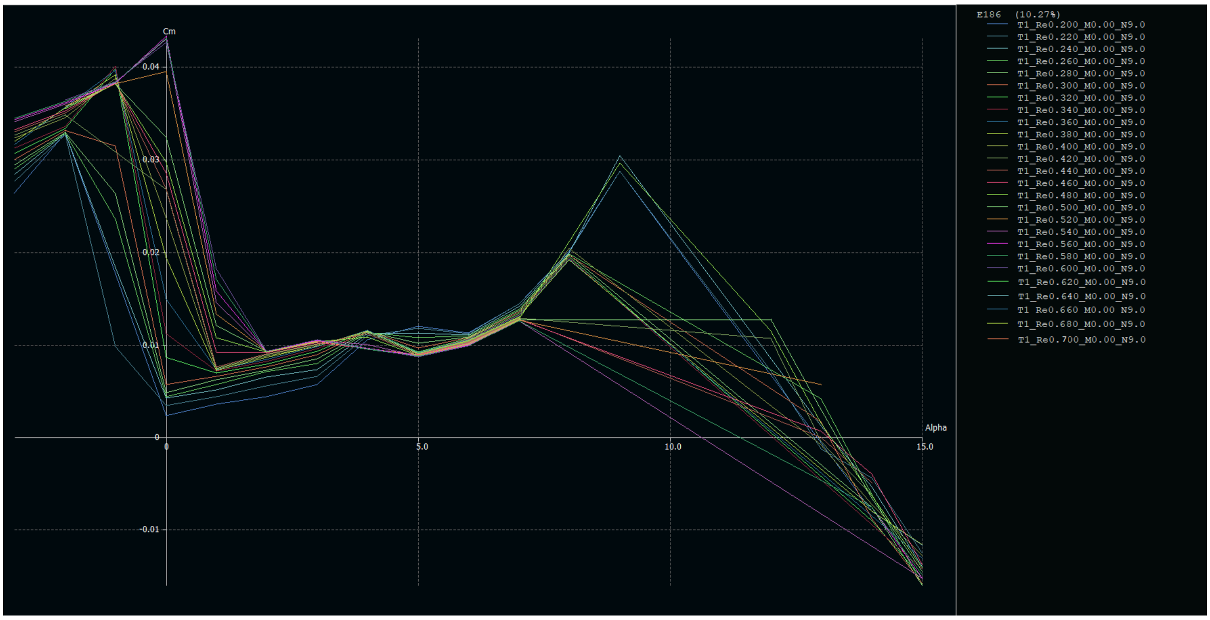

Figure A.3.: Eppler186 Cm – Alpha graph for different Reynolds values, obtained from XFLR5

	y (m)	chord (m)	offset (m)	dihedral	twist(°)	foil	X-panels	X-dist	Y-panels	Y-dist
1	0,000	0,890	0,000	0,0	0,00	E186 (10.27%)	20	Cosine	20	Uniform
2	0,150	0,740	0,150	0,0	0,00	E186 (10.27%)	20	Cosine	20	Uniform
3	0,450	0,400	0,400	0,0	-0,30	MH 45 9.85%	20	Cosine	20	Uniform
4	1,200	0,180	0,900	0,0	-0,60	MH 45 9.85%	20	Cosine	20	Uniform
5	1,200	0,180	0,900	90,0	-0,60	NACA-0009 9.0% smoothed	20	Cosine	20	Uniform
6	1,300	0,100	1,000		0,00	NACA-0009 9.0% smoothed				

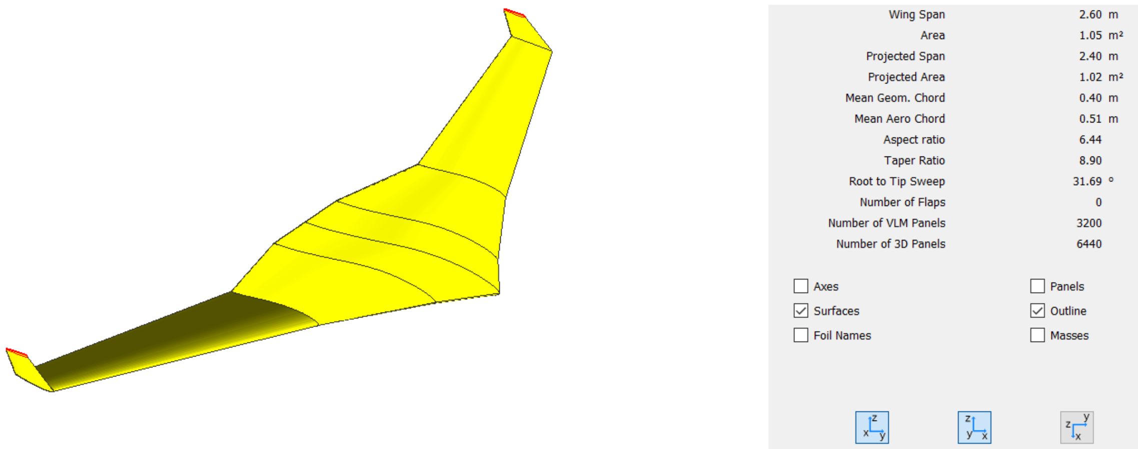

Figure A.4.: Geometric design of the flying wing

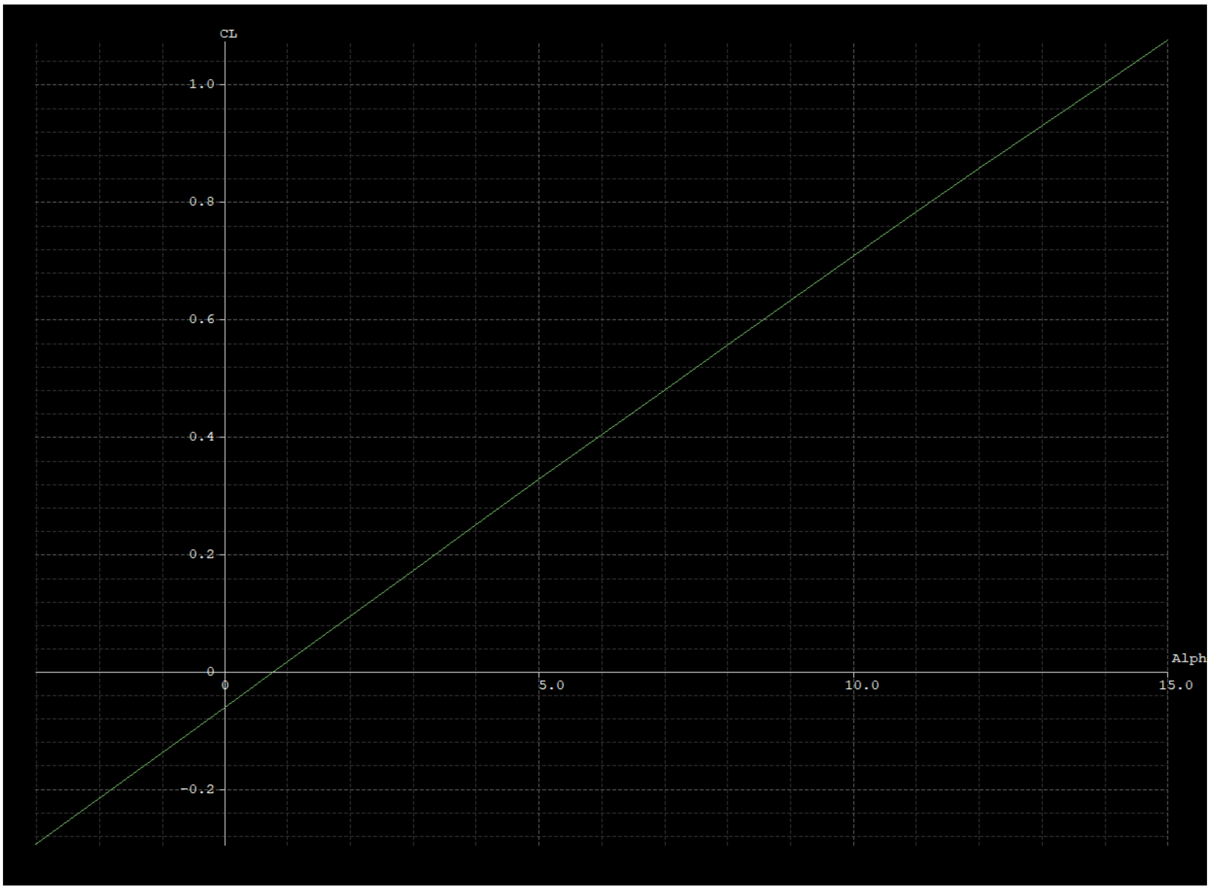

Figure A.5.: CL – Alpha graph of the Flying wing

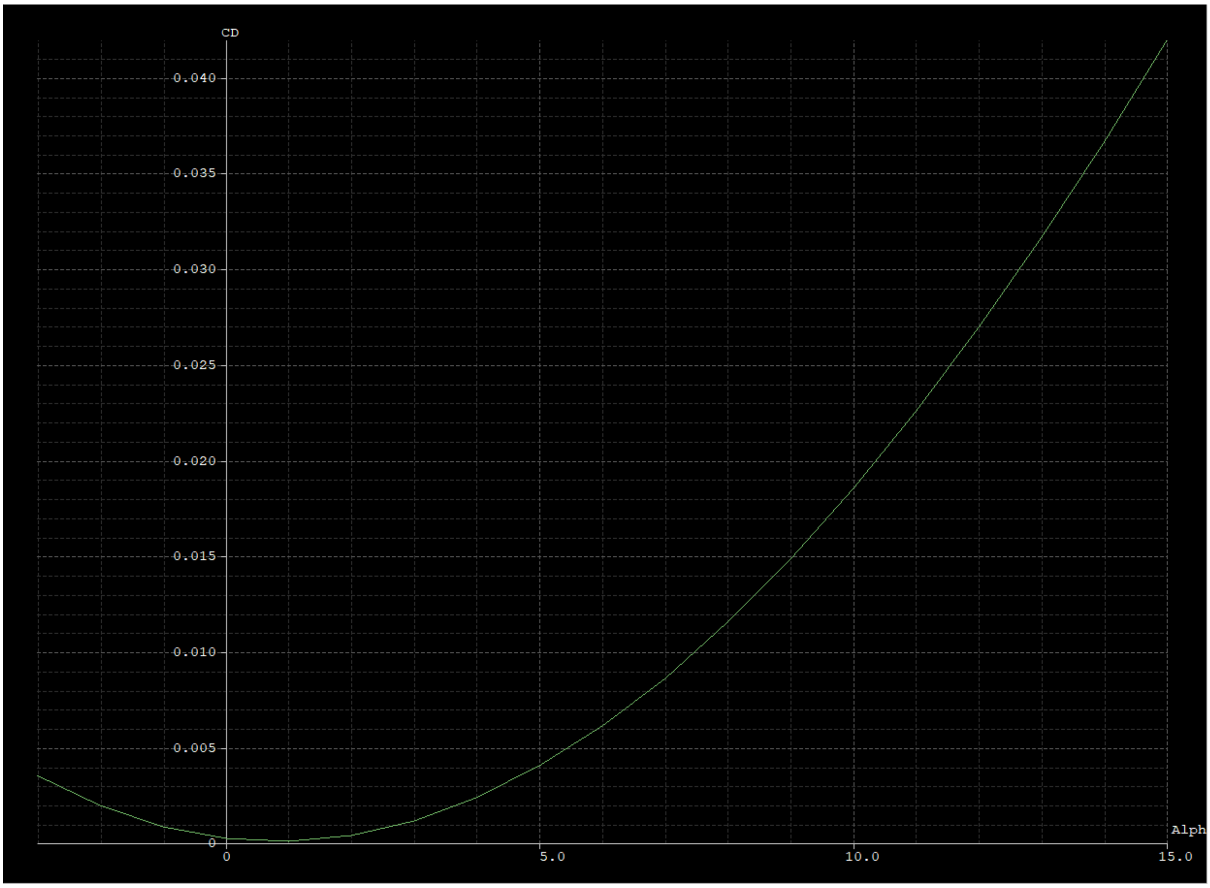

Figure A.6.: CD – Alpha graph of the Flying wing

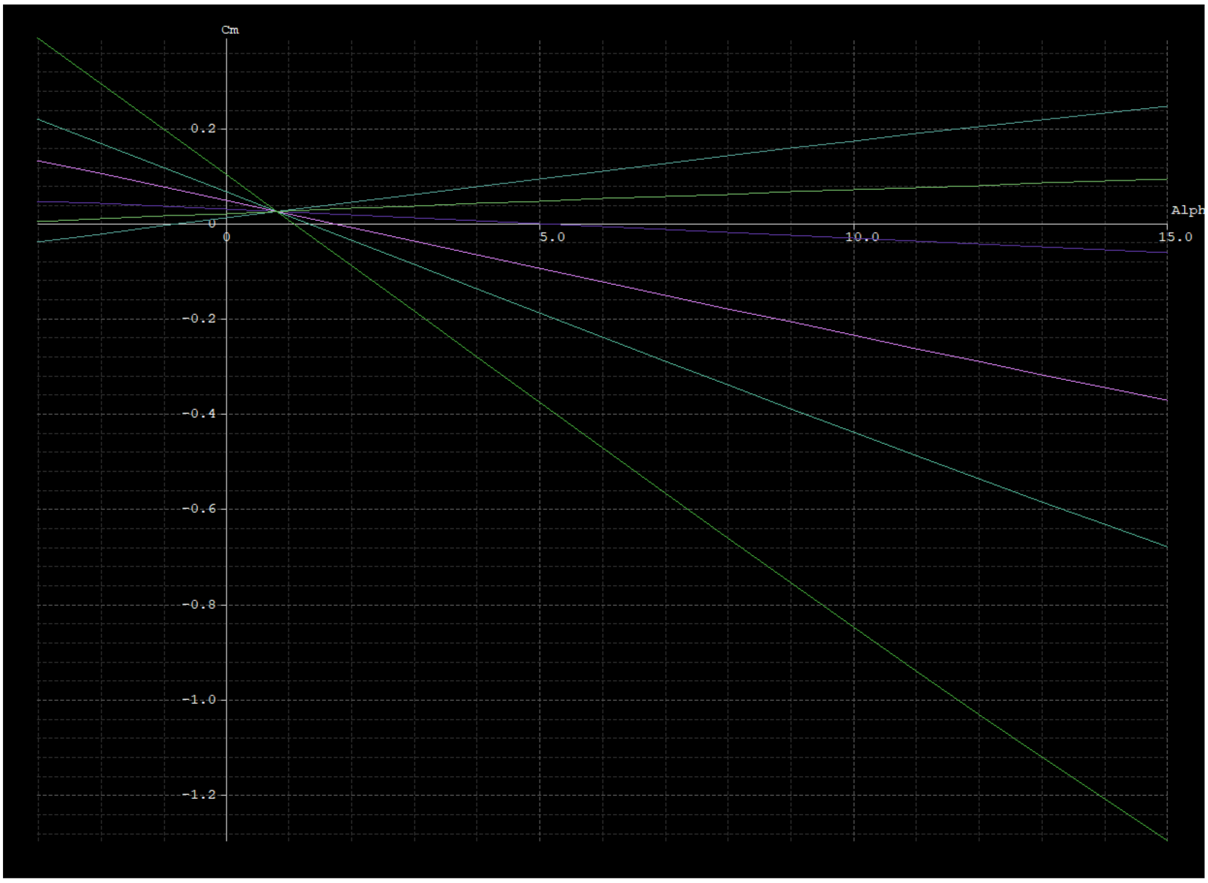

Figure A.7.: CM – Alpha graph of the Flying wing

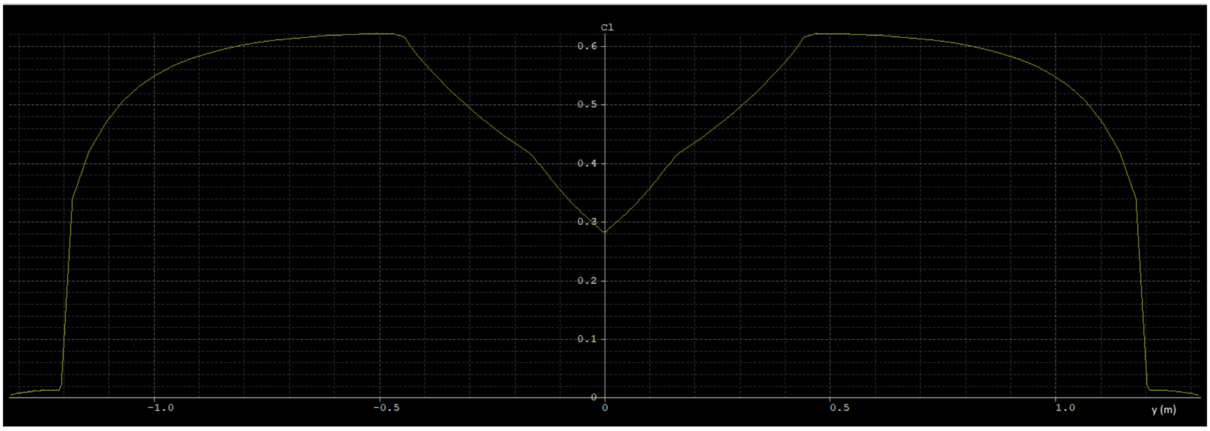

Figure A.8.: CL distribution for Alpha = 4º

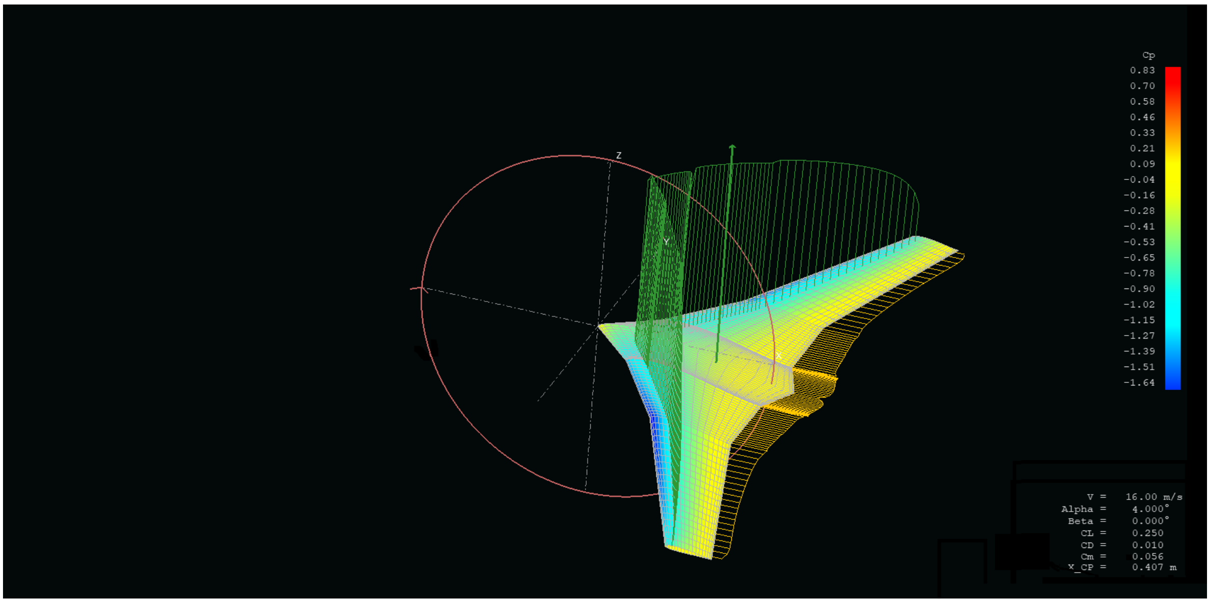

Figure A.9.: Flying wing at static analysis and pitching moment. at alpha 4^{o}

Numerical Simulation by CFD

A.3.1 Simulation parameters

Axis	Minimum (m)	Maximum (m)
X-coordinate	-1.13118	2.827659
Y-coordinate	-3.439945	3.439945
Z-coordinate	-1.024849	1.078300

Table A.1.: Domain Extents

Minimum Volume (m^3)	Maximum Volume (m^3)	Total Volume (m^3)
$2.430786 \cdot 10^{-13}$	$8.733648 \cdot 10^{-3}$	$5.476718 \cdot 10$

Table A.2.: Volume statistics

The face area statistics are:

- The Minimum Face Area is $4.854192 \cdot 10^{-9} m^2$
- The Maximum Face Area is $1.084398 \cdot 10^{-1} m^2$

Zone	Elements
1	25604 triangular wall faces
2	1864131 triangular interior faces
3	939390 tetrahedral cells
6	326 triangular wall faces
7	316 triangular velocity-inlet faces
8	304 triangular pressure-outlet faces
9	636 triangular wall faces
10	666 triangular wall faces
11	1446 triangular wall faces
Total nodes	164202 nodes
Total faces	1893429 faces
Total cells	939390 cells

Table A.3.: Meshing size for each zone

Mesh Quality:

- Orthogonal Quality ranges from 0 to 1, where values close to 0 correspond to low quality.
- The Minimum Orthogonal Quality is $1.41843 \cdot 10^{-1}$
- The Maximum Aspect Ratio is $3.70990 \cdot 10$

Element name	Type /Condition	Parameters
Wall_right	Wall	Static Pressure
Wall_left	Wall	Static Pressure
Frontal_inlet	Velocity inlet	Airspeed (16m/s) by components
Back_outlet	Pressure outlet	Pressure and velocity as output
Top_wall	Wall	Static Pressure
Bottom_wall	Wall	Static Pressure
Wall-solid	Body	Null normal velocity component to the surface

Table A.4.: Boundary conditions for all the elements

A.3.2 Simulation results

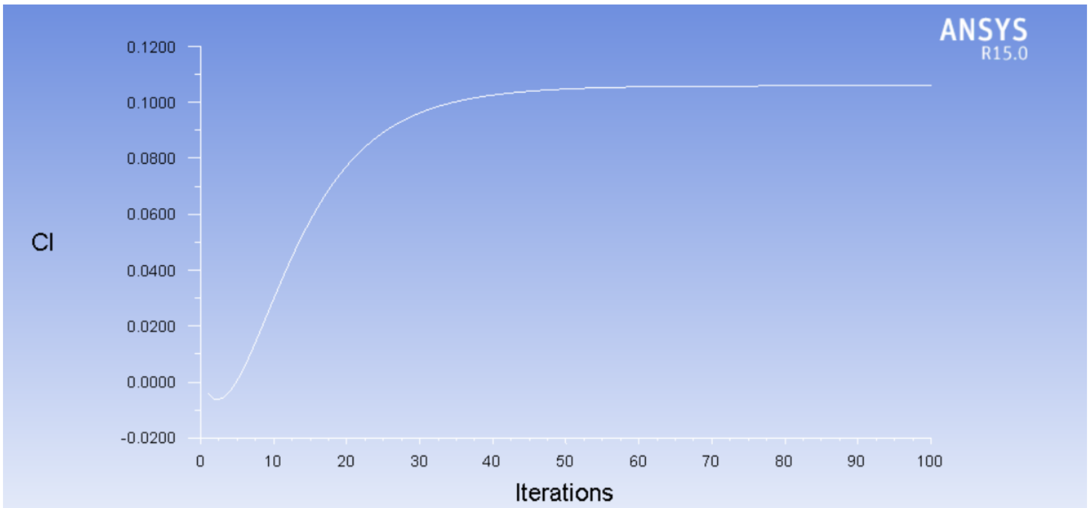

Figure A.10.: Wing Lift Coefficient for $\alpha = 1°$

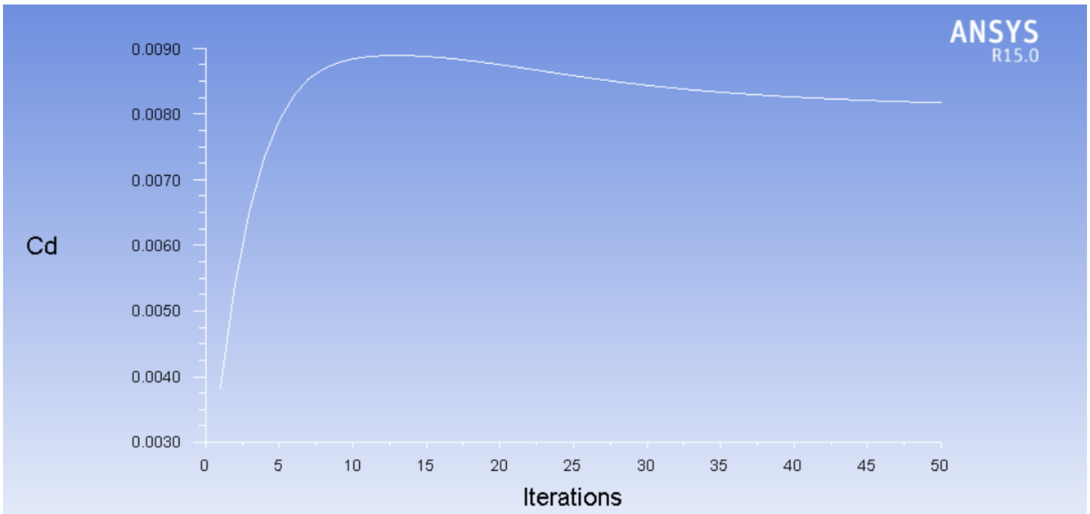

Figure A.11.: Wing Drag Coefficient for $\alpha = 1°$

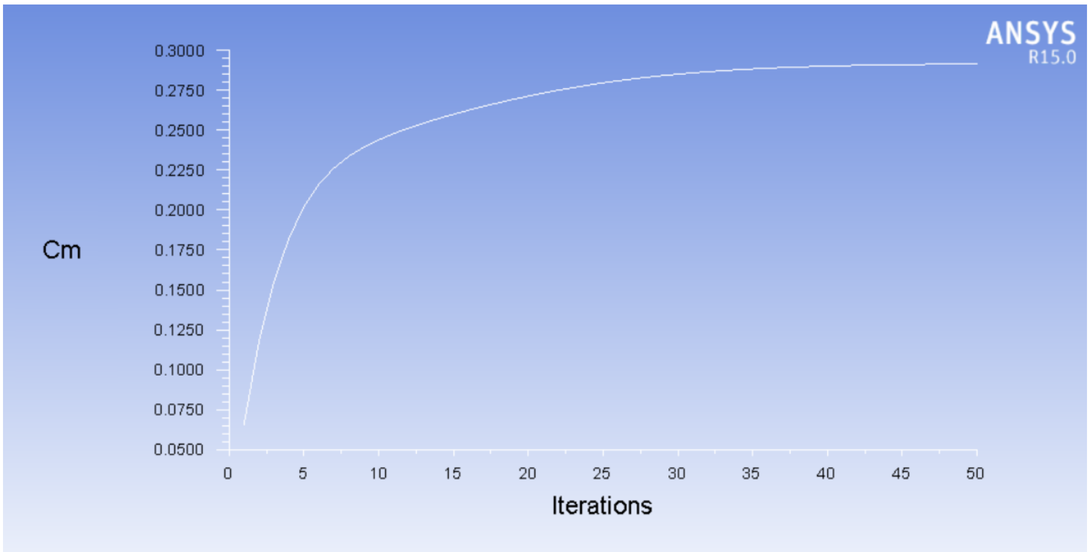

Figure A.12.: Wing Pitch moment Coefficient for $\alpha = 1°$

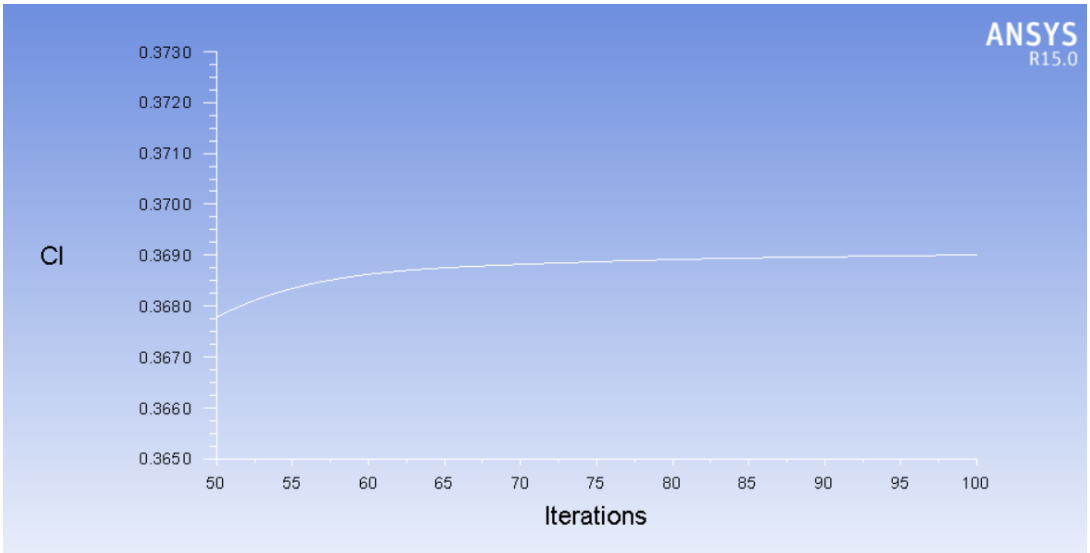

Figure A.13.: Wing Lift Coefficient for $\alpha = 4°$

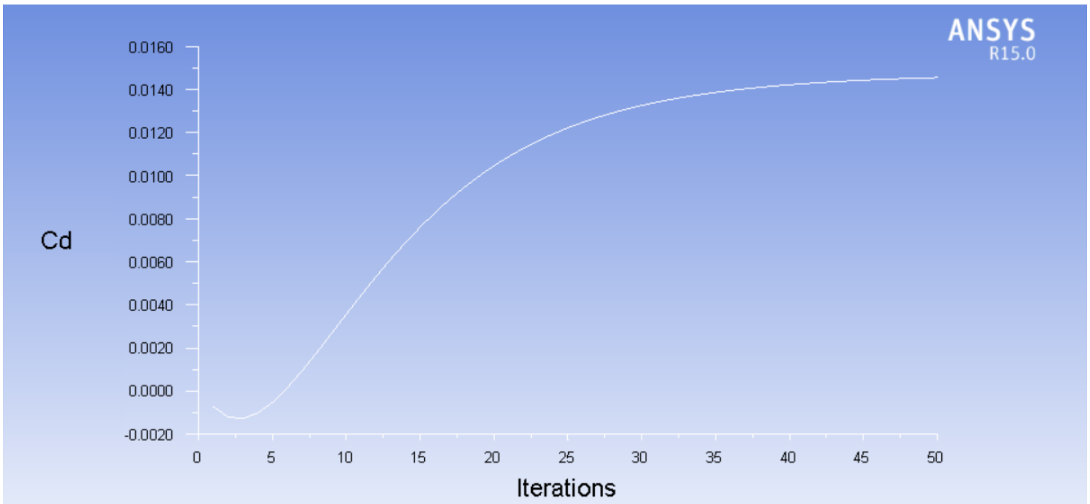

Figure A.14.: Wing Drag Coefficient for $\alpha = 4°$

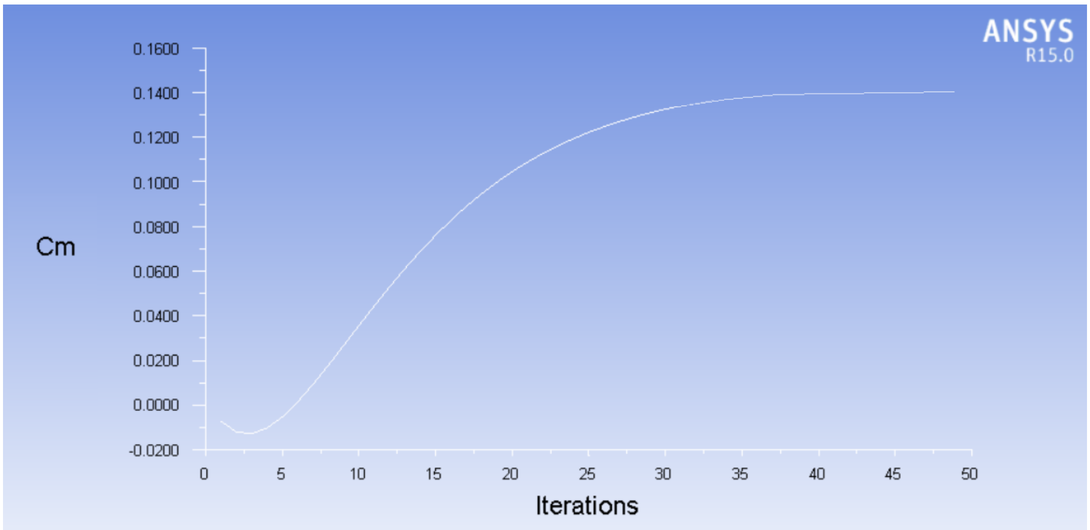

Figure A.15.: Wing Pitch moment Coefficient for $\alpha = 4°$

$\alpha(deg)$	C_L	C_D	C_M
-10	-0.5759	0.1054	0.8800
-9	-0.6128	0.0867	0.8211
-8	-0.6228	0.0703	0.7517
-7	-0.5668	0.0560	0.6814
-6	-0.4905	0.0455	0.6351
-5	-0.4077	0.0345	0.6015
-4	-0.3271	0.0204	0.5662
-3	-0.2430	0.0130	0.5155
-2	-0.1623	0.0111	0.4814
-1	-0.0680	0.0082	0.4164
0	0.0215	0.0079	0.3458
1	0.1068	0.0084	0.2998
2	0.1872	0.0088	0.2598
3	0.2697	0.0108	0.1998
4	0.3691	0.0145	0.1401
5	0.4501	0.0191	0.0818
6	0.5382	0.0257	0.0350
7	0.6181	0.0357	-0.0006
8	0.6988	0.0441	-0.0256
9	0.7777	0.0529	-0.0506
10	0.8577	0.0621	-0.0756
11	0.9298	0.0702	-0.1006
12	0.9981	0.0800	-0.1256
13	1.0577	0.0930	-0.1506
14	1.0930	0.1101	-0.1756
15	1.0658	0.1307	-0.1986
16	1.0010	0.1475	-0.2304
17	0.9260	0.1671	-0.2669

Table A.5.: Aerodynamic coefficients obtained from Fluent Simulation

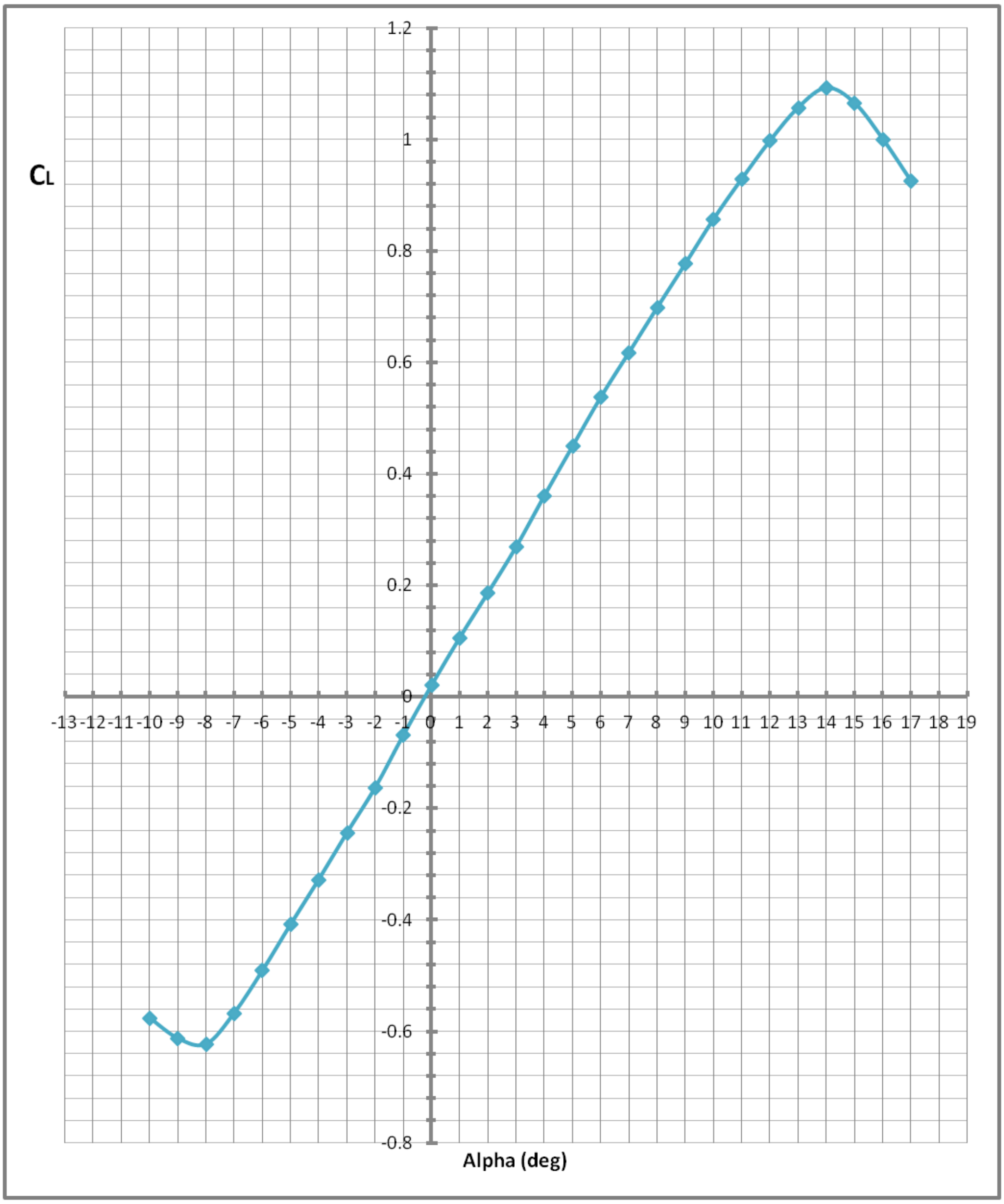

Figure A.16.: Lift coefficient vs AoA

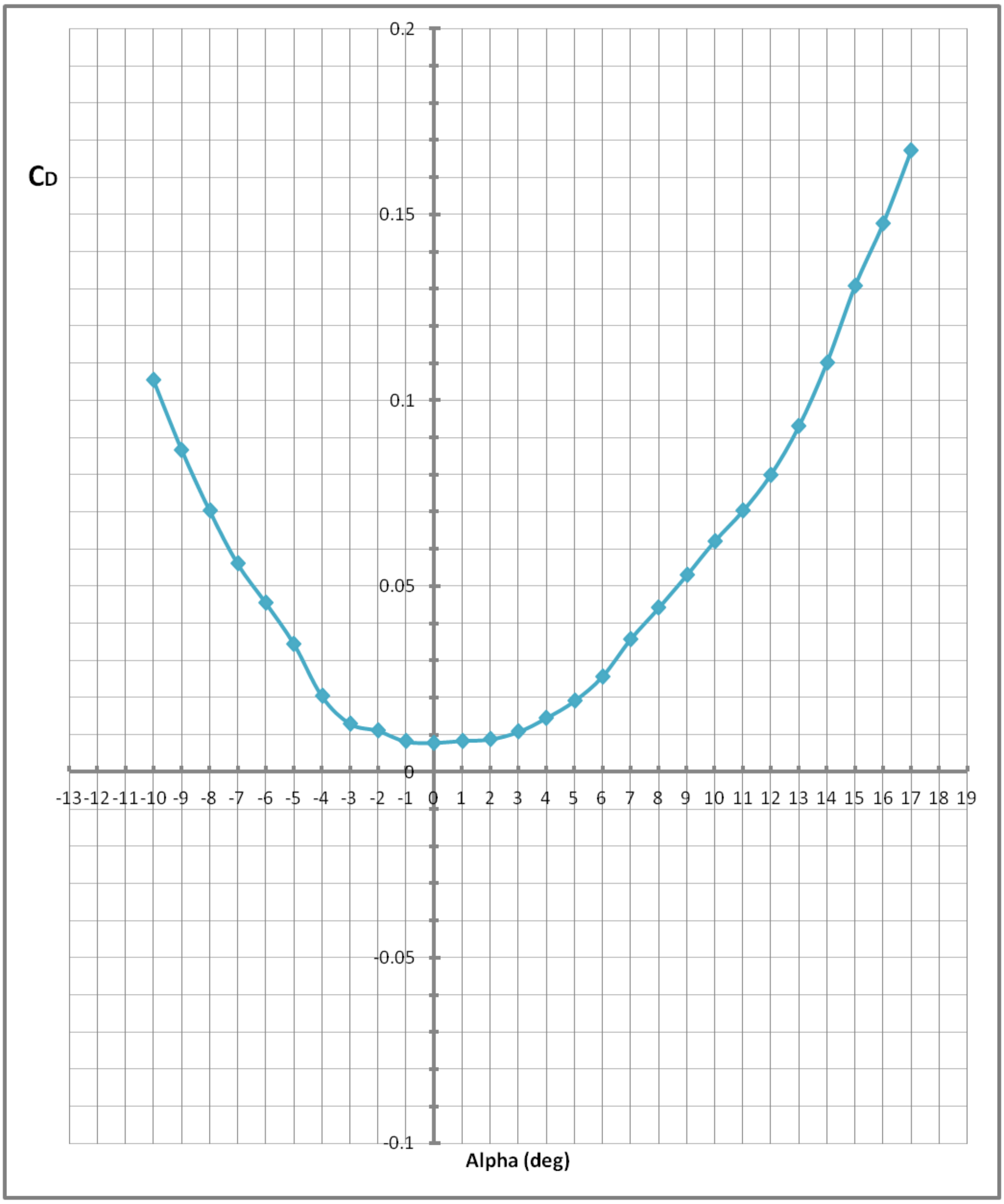

Figure A.17.: Drag coefficient vs AoA

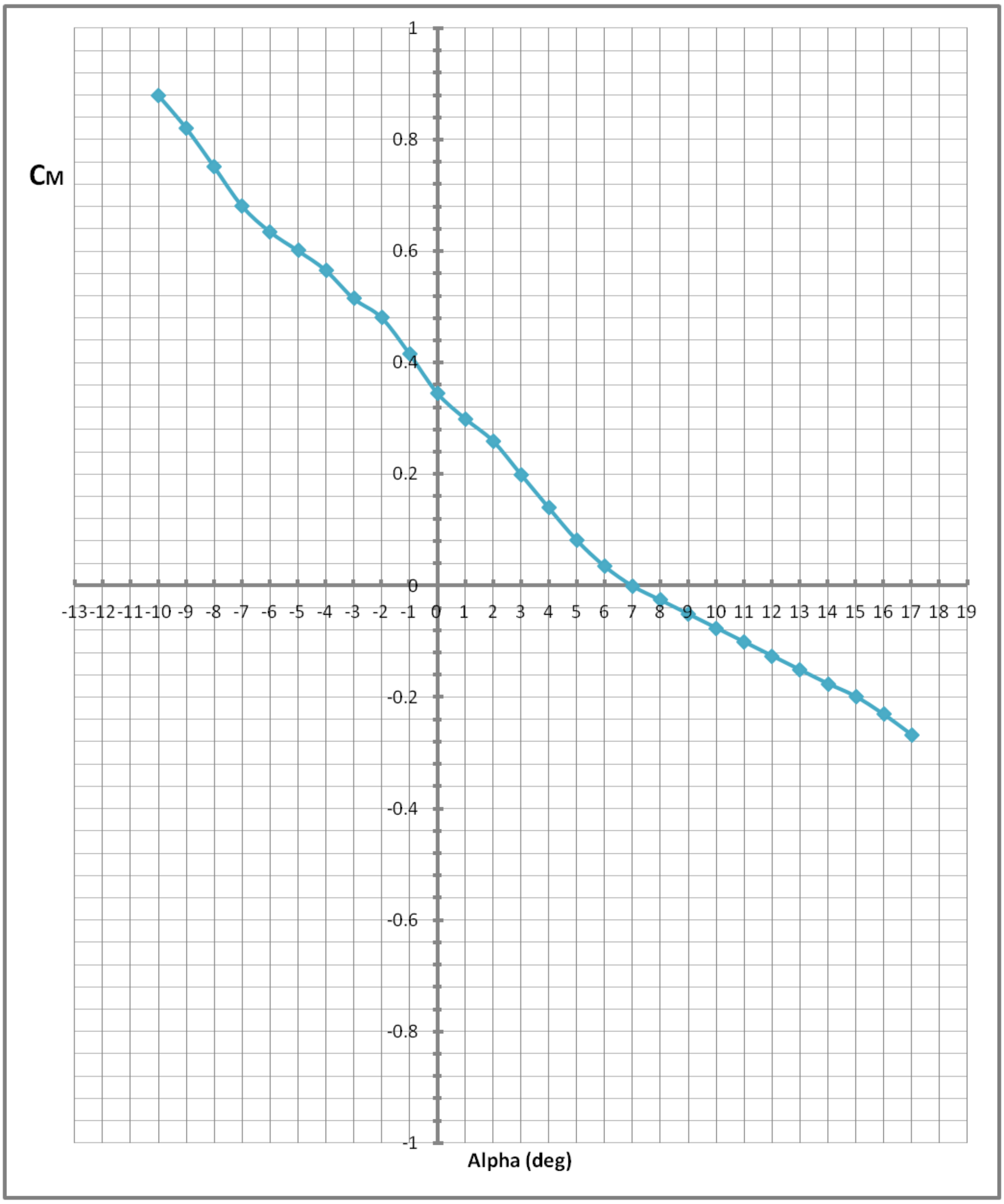

Figure A.18.: Pitch moment coefficient vs AoA

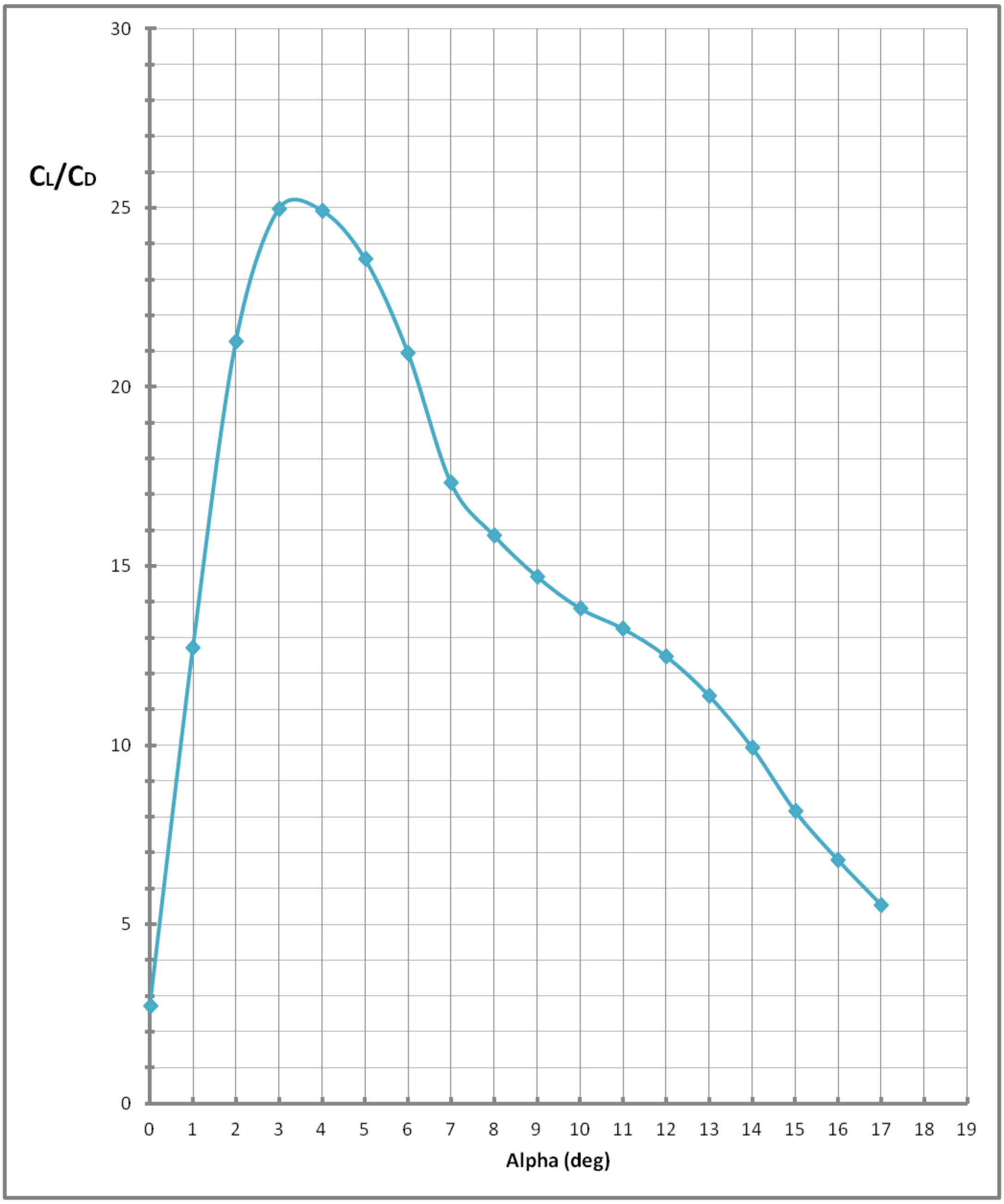

Figure A.19.: Lift to Drag ratio vs AoA

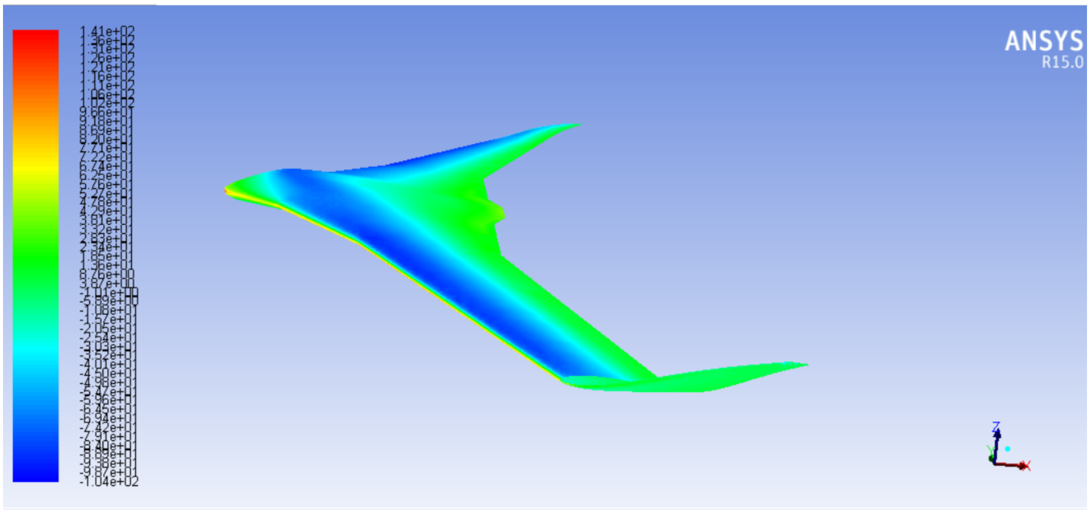

Figure A.20.: Miscellaneous: Pressure distribution map

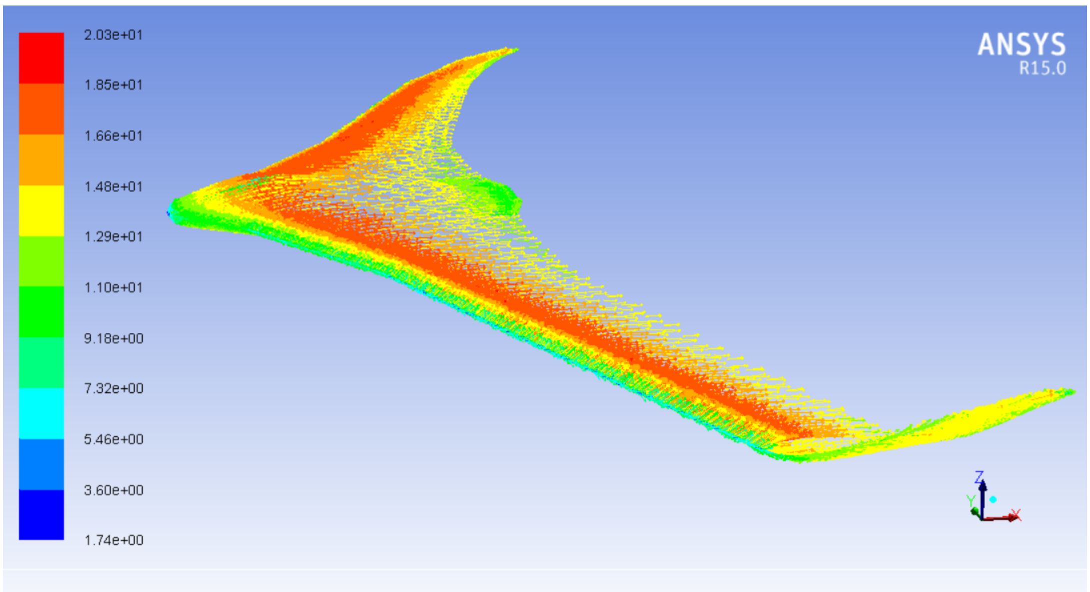

Figure A.21.: Miscellaneous: Path lines colored by relative velocity (particle tracking)

Part B

PROPULSION

Introduction

This chapter provides more details regarding the blade element method calculations as an extension of what has already been explained in the project Report.

Blade Element Method

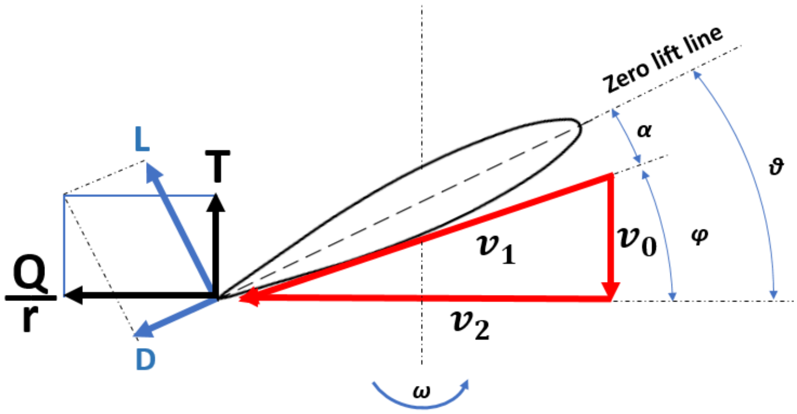

Figure B.1.: Force and speed components on a blade element

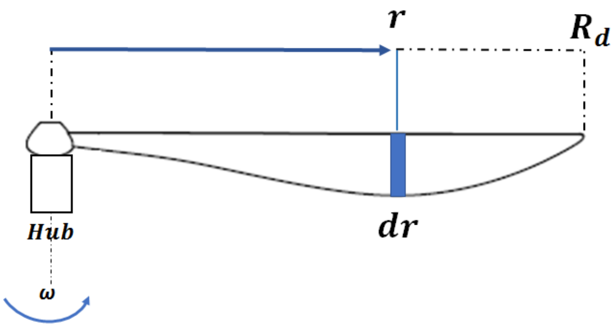

Figure B.2.: Blade element scheme

Considering $\theta(r)$ as the twist distribution along the propeller radius and the speed components as shown in the previous figure, where v_0 is the **axial flow at propeller disk** and v_2 is the **angular flow**, the angle of attack of each blade element can be written as:

$$\alpha(r) = \theta(r) - \phi(r) = \theta(r) - \arctan\left(\frac{v_0}{v_2}\right) \tag{B.2.1}$$

It is important to note that:

- 2D study is considered, so the induced velocity components are neglected along the blade radius
- for each blade, the angle of attack is measured regarding the airfoil zero lift line

Therefore, for a given **twist distribution** $\theta(r)$, the local angle of attack for each blade can be calculated, and from the airfoil polar graphs the corresponding c_l and c_d values can be found. Then, for each blade element, the total lift and drag forces can be determined, which should be projected on the axial and tangential axis, to determine thrust and torque components:

$$\Delta T = \Delta L \cos\phi - \Delta D \sin\phi \tag{B.2.2}$$

$$\frac{\Delta Q}{r} = \Delta L \sin\phi + \Delta D \cos\phi \tag{B.2.3}$$

where:

$$\Delta L = c_l \cdot \frac{1}{2} \cdot \rho \cdot {v_1}^2 \cdot c \cdot dr \tag{B.2.4}$$

and

$$\Delta D = c_d \cdot \frac{1}{2} \cdot \rho \cdot {v_1}^2 \cdot c \cdot dr \tag{B.2.5}$$

where

$$v_1 = \sqrt{{v_0}^2 + {v_2}^2} \tag{B.2.6}$$

Considering that the propeller has two blades:

$$\Delta T = \frac{1}{2}\rho {v_1}^2 c(c_l \cos\phi - c_d \sin\phi) dr \cdot 2 \tag{B.2.7}$$

$$\Delta Q = \frac{1}{2}\rho {v_1}^2 c(c_d \cos\phi + c_l \sin\phi) r \cdot dr \cdot 2 \tag{B.2.8}$$

Therefore, the design steps would be defined as:

- definition of the twist distribution $\theta(r)$
- discretization of the blade into N elements along the radius
- calculation of the angle of attack of each blade element $\alpha(r)$
- determination of c_l and c_d for each blade element
- determination of the local drag and lift, and then, local thrust and torque

B.2.1 BEM without inflow factors

At this section, the axial flow at propeller disk v_0 and the angular flow v_2 are calculated neglecting the inflow factors. Therefore, the axial flow can be considered approximately equal to the aircraft advance speed and the angular flow can be calculated considering only the blade rotation.

$$v_0 = u_\infty$$

$$v_2 = \omega \cdot r$$

$$v_1 = \sqrt{{v_o}^2 + {v_2}^2} = \sqrt{{u_\infty}^2 + \omega \cdot r^2}$$

According to [7] and Alfred Gessow studies (1948), the ideal twist can be calculated as:

$$\theta(r) = \frac{\theta_{tip}}{r} \tag{B.2.9}$$

Actually, the state of the art of the aircraft propellers suggests that the ideal theoretical twist is almost identical to the optimal twist, based on the wind tunnel analysis [7]. Furthermore, the Eppler E63 airfoil has been selected for the blade design, which is one of the most used airfoils for medium size propellers. The next calculations will be done for take-off, since it is when the propulsive efficiency seems to be the lowest according to the previous chapter. For the next calculations, 6000 RPM will be considered. The blade tip angular flow is calculated with the next equation, for take-off and cruise flight:

$$v_{1tip_{t-o}} = \sqrt{{u_\infty}^2 + \omega \cdot {R_d}^2} = \sqrt{9.84^2 + \left(6000 \cdot \frac{2\pi}{60} \cdot 0.2\right)^2} = 126.05\ [m/s]$$

$$\phi_{tip_{t-o}} = \arcsin \frac{u_\infty}{v_1} \rightarrow \phi_{tip} = 4.48°$$

and

$$v_{1tip_{cr}} = \sqrt{{u_\infty}^2 + \omega \cdot {R_d}^2} = \sqrt{16^2 + \left(6000 \cdot \frac{2\pi}{60} \cdot 0.2\right)^2} = 126.7\ [m/s]$$

$$\phi_{tip_{cr}} = \arcsin \frac{u_\infty}{v_1} \rightarrow \phi_{tip} = 7.25°$$

At cruise flight condition, the higher ϕ for the same twist distribution will decrease the angle of attack. Therefore, for the calculation of the θ_{tip}, $\phi_{tip_{cr}}$ will be considered as the reference value. Considering the Eppler E63 airfoil c_l/c_d vs α graph for Reynolds numbers between 50,000 and 100,000, since the maximum Reynolds over the blade is around 77000, the optimal α value is obtained, which is around $\alpha_{opt} = 5°$. Therefore, the blade twist at the tip is:

$$\theta_{tip} = \alpha_{opt} + \phi_{tip} = 12.25°$$

Then, the blade is divided into 100 elements. The twist distribution $\theta(r)$ for $0.14m < r < 0.2m$ is calculated according to the ideal twist equation, while for $0 < r < 0.14m$ linear twist distribution is selected, which provides almost constant angle of attack distribution and values close to α_{opt}. The next tables are generated, for both, take-off and cruise flight conditions:

Element	r [m]	$\frac{r}{R_d}$	dr [m]	c [m]	V_0 [m/s]	V_2 [m/s]	V_1 [m/s]	ϕ	θ	α	$\alpha°$	C_l	C_d	ΔT	ΔQ
1	0.0134	0.0672	0.0019	0.0450	9.84	8.44	12.97	0.8617	1.1052	0.2436	13.96	2.2339	0.1991		
2	0.0153	0.0766	0.0019	0.0429	9.84	9.62	13.76	0.7966	1.0394	0.2428	13.91	2.2273	0.1982		
3	0.0172	0.0859	0.0019	0.0427	9.84	10.80	14.61	0.7390	0.9921	0.2531	14.50	2.3104	0.2101		
4	0.0191	0.0953	0.0019	0.0424	9.84	11.98	15.50	0.6877	0.9432	0.2555	14.64	2.3291	0.2127		
5	0.0209	0.1047	0.0019	0.0422	9.84	13.16	16.43	0.6422	0.8977	0.2554	14.64	2.3291	0.2127		
6	0.0228	0.1141	0.0019	0.0419	9.84	14.33	17.39	0.6016	0.8603	0.2587	14.82	2.3549	0.2164		
7	0.0247	0.1234	0.0019	0.0417	9.84	15.51	18.37	0.5653	0.8159	0.2506	14.36	2.2901	0.2072		
8	0.0266	0.1328	0.0019	0.0414	9.84	16.69	19.37	0.5327	0.7793	0.2466	14.13	2.2579	0.2026		
9	0.0284	0.1422	0.0019	0.0412	9.84	17.87	20.40	0.5034	0.7503	0.2469	14.15	2.2606	0.2029		
10	0.0303	0.1516	0.0019	0.0409	9.84	19.05	21.44	0.4769	0.7137	0.2368	13.57	2.1797	0.1914		
11	0.0322	0.1609	0.0019	0.0407	9.84	20.22	22.49	0.4528	0.6843	0.2315	13.26	2.1368	0.1853		
12	0.0341	0.1703	0.0019	0.0404	9.84	21.40	23.56	0.4309	0.6620	0.2310	13.24	2.1330	0.1847		
13	0.0359	0.1797	0.0019	0.0401	9.84	22.58	24.63	0.4110	0.6365	0.2255	12.92	2.0888	0.1784		
14	0.0378	0.1891	0.0019	0.0399	9.84	23.76	25.72	0.3927	0.6127	0.2200	12.61	2.0449	0.1721		
15	0.0397	0.1984	0.0019	0.0396	9.84	24.94	26.81	0.3758	0.5955	0.2196	12.58	2.0417	0.1717		
16	0.0416	0.2078	0.0019	0.0394	9.84	26.11	27.91	0.3603	0.5697	0.2093	11.99	1.9592	0.1599	0.0626	0.0012
17	0.0434	0.2172	0.0019	0.0391	9.84	27.29	29.01	0.3460	0.5502	0.2042	11.70	1.9180	0.1540	0.0663	0.0013
18	0.0453	0.2266	0.0019	0.0389	9.84	28.47	30.12	0.3328	0.5370	0.2042	11.70	1.9182	0.1540	0.0714	0.0014
19	0.0472	0.2359	0.0019	0.0386	9.84	29.65	31.24	0.3204	0.5149	0.1944	11.14	1.8395	0.1428	0.0736	0.0015
20	0.0491	0.2453	0.0019	0.0384	9.84	30.83	32.36	0.3090	0.4988	0.1898	10.87	1.8023	0.1375	0.0773	0.0015
21	0.0509	0.2547	0.0019	0.0381	9.84	32.00	33.48	0.2983	0.4886	0.1903	10.90	1.8065	0.1381	0.0828	0.0017
22	0.0528	0.2641	0.0019	0.0379	9.84	33.18	34.61	0.2883	0.4843	0.1960	11.23	1.8523	0.1446	0.0904	0.0018
23	0.0547	0.2734	0.0019	0.0376	9.84	34.36	35.74	0.2789	0.4708	0.1919	10.99	1.8191	0.1399	0.0944	0.0019
24	0.0566	0.2828	0.0019	0.0374	9.84	35.54	36.88	0.2701	0.4630	0.1929	11.05	1.8275	0.1411	0.1006	0.0021
25	0.0584	0.2922	0.0019	0.0371	9.84	36.72	38.01	0.2618	0.4459	0.1841	10.55	1.7568	0.1310	0.1024	0.0021
26	0.0603	0.3016	0.0019	0.0369	9.84	37.90	39.15	0.2541	0.4345	0.1805	10.34	1.7275	0.1268	0.1064	0.0022
27	0.0622	0.3109	0.0019	0.0366	9.84	39.07	40.29	0.2467	0.4287	0.1820	10.43	1.7395	0.1285	0.1130	0.0023
28	0.0641	0.3203	0.0019	0.0364	9.84	40.25	41.44	0.2398	0.4133	0.1736	9.95	1.6724	0.1189	0.1144	0.0024
29	0.0659	0.3297	0.0019	0.0361	9.84	41.43	42.58	0.2332	0.4035	0.1704	9.76	1.6465	0.1152	0.1184	0.0024
30	0.0678	0.3391	0.0019	0.0358	9.84	42.61	43.73	0.2270	0.3992	0.1723	9.87	1.6618	0.1174	0.1254	0.0026
31	0.0697	0.3484	0.0019	0.0356	9.84	43.79	44.88	0.2211	0.3853	0.1643	9.41	1.5978	0.1083	0.1264	0.0026
32	0.0716	0.3578	0.0019	0.0353	9.84	44.96	46.03	0.2154	0.4019	0.1864	10.68	1.7754	0.1336	0.1467	0.0031
33	0.0734	0.3672	0.0019	0.0351	9.84	46.14	47.18	0.2101	0.3988	0.1887	10.81	1.7934	0.1362	0.1548	0.0033
34	0.0753	0.3766	0.0019	0.0348	9.84	47.32	48.33	0.2050	0.3861	0.1810	10.37	1.7321	0.1274	0.1561	0.0034
35	0.0772	0.3859	0.0019	0.0346	9.84	48.50	49.49	0.2002	0.3787	0.1785	10.23	1.7117	0.1245	0.1607	0.0035
36	0.0791	0.3953	0.0019	0.0343	9.84	49.68	50.64	0.1956	0.3766	0.1810	10.37	1.7322	0.1275	0.1693	0.0037
37	0.0809	0.4047	0.0019	0.0341	9.84	50.85	51.80	0.1911	0.3648	0.1737	9.95	1.6732	0.1190	0.1701	0.0037
38	0.0828	0.4141	0.0019	0.0338	9.84	52.03	52.95	0.1869	0.3583	0.1714	9.82	1.6550	0.1164	0.1748	0.0038
39	0.0847	0.4234	0.0019	0.0336	9.84	53.21	54.11	0.1829	0.3571	0.1742	9.98	1.6776	0.1197	0.1838	0.0040
40	0.0866	0.4328	0.0019	0.0333	9.84	54.39	55.27	0.1790	0.3461	0.1671	9.58	1.6206	0.1115	0.1841	0.0040
41	0.0884	0.4422	0.0019	0.0331	9.84	55.57	56.43	0.1753	0.3404	0.1651	9.46	1.6043	0.1092	0.1887	0.0041
42	0.0903	0.4516	0.0019	0.0328	9.84	56.75	57.59	0.1717	0.3398	0.1681	9.63	1.6286	0.1127	0.1981	0.0044
43	0.0922	0.4609	0.0019	0.0326	9.84	57.92	58.75	0.1683	0.3295	0.1612	9.24	1.5733	0.1048	0.1979	0.0044
44	0.0941	0.4703	0.0019	0.0323	9.84	59.10	59.91	0.1650	0.3244	0.1594	9.13	1.5586	0.1027	0.2025	0.0045
45	0.0959	0.4797	0.0019	0.0320	9.84	60.28	61.08	0.1618	0.3244	0.1626	9.32	1.5846	0.1064	0.2124	0.0047
46	0.0978	0.4891	0.0019	0.0318	9.84	61.46	62.24	0.1588	0.3147	0.1559	8.93	1.5307	0.0987	0.2116	0.0047
47	0.0997	0.4984	0.0019	0.0315	9.84	62.64	63.40	0.1558	0.3101	0.1543	8.84	1.5175	0.0968	0.2161	0.0048
48	0.1016	0.5078	0.0019	0.0313	9.84	63.81	64.57	0.1530	0.3107	0.1577	9.03	1.5447	0.1007	0.2264	0.0051
49	0.1034	0.5172	0.0019	0.0310	9.84	64.99	65.73	0.1503	0.3014	0.1511	8.66	1.4922	0.0932	0.2251	0.0050
50	0.1053	0.5266	0.0019	0.0308	9.84	66.17	66.90	0.1476	0.2972	0.1496	8.57	1.4802	0.0915	0.2295	0.0051
51	0.1072	0.5359	0.0019	0.0305	9.84	67.35	68.06	0.1451	0.2982	0.1532	8.78	1.5086	0.0955	0.2402	0.0054
52	0.1091	0.5453	0.0019	0.0303	9.84	68.53	69.23	0.1426	0.2894	0.1468	8.41	1.4572	0.0882	0.2383	0.0054
53	0.1109	0.5547	0.0019	0.0300	9.84	69.70	70.40	0.1402	0.2856	0.1454	8.33	1.4462	0.0866	0.2426	0.0055

Element	r [m]	$\frac{r}{R_d}$	dr [m]	c [m]	V_0 [m/s]	V_2 [m/s]	V_1 [m/s]	ϕ	θ	α	α°	C_l	C_d	ΔT	ΔQ
54	0.1128	0.5641	0.0019	0.0298	9.84	70.88	71.56	0.1379	0.2870	0.1491	8.54	1.4757	0.0908	0.2537	0.0058
55	0.1147	0.5734	0.0019	0.0295	9.84	72.06	72.73	0.1357	0.2785	0.1428	8.18	1.4253	0.0836	0.2512	0.0057
56	0.1166	0.5828	0.0019	0.0293	9.84	73.24	73.90	0.1336	0.2751	0.1415	8.11	1.4153	0.0822	0.2554	0.0058
57	0.1184	0.5922	0.0019	0.0290	9.84	74.42	75.06	0.1315	0.2768	0.1453	8.33	1.4456	0.0865	0.2669	0.0061
58	0.1203	0.6016	0.0019	0.0288	9.84	75.59	76.23	0.1294	0.2686	0.1391	7.97	1.3961	0.0794	0.2637	0.0060
59	0.1222	0.6109	0.0019	0.0285	9.84	76.77	77.40	0.1275	0.2655	0.1380	7.91	1.3869	0.0781	0.2678	0.0061
60	0.1241	0.6203	0.0019	0.0283	9.84	77.95	78.57	0.1256	0.2674	0.1419	8.13	1.4181	0.0826	0.2797	0.0064
61	0.1259	0.6297	0.0019	0.0280	9.84	79.13	79.74	0.1237	0.2595	0.1358	7.78	1.3692	0.0756	0.2759	0.0063
62	0.1278	0.6391	0.0019	0.0277	9.84	80.31	80.91	0.1219	0.2567	0.1347	7.72	1.3608	0.0744	0.2798	0.0064
63	0.1297	0.6484	0.0019	0.0275	9.84	81.49	82.08	0.1202	0.2589	0.1387	7.95	1.3927	0.0790	0.2921	0.0068
64	0.1316	0.6578	0.0019	0.0272	9.84	82.66	83.25	0.1185	0.2512	0.1327	7.60	1.3445	0.0721	0.2876	0.0066
65	0.1334	0.6672	0.0019	0.0270	9.84	83.84	84.42	0.1168	0.2486	0.1317	7.55	1.3367	0.0710	0.2914	0.0067
66	0.1353	0.6766	0.0019	0.0267	9.84	85.02	85.59	0.1152	0.2510	0.1358	7.78	1.3692	0.0756	0.3039	0.0071
67	0.1372	0.6859	0.0019	0.0265	9.84	86.20	86.76	0.1137	0.2435	0.1299	7.44	1.3217	0.0688	0.2988	0.0069
68	0.1391	0.6953	0.0019	0.0262	9.84	87.38	87.93	0.1121	0.2411	0.1290	7.39	1.3145	0.0678	0.3024	0.0069
69	0.1409	0.7047	0.0019	0.0260	9.84	88.55	89.10	0.1107	0.2838	0.1731	9.92	1.6684	0.1183	0.3896	0.0101
70	0.1428	0.7141	0.0019	0.0257	9.84	89.73	90.27	0.1092	0.2994	0.1902	10.90	1.8056	0.1379	0.4284	0.0115
71	0.1447	0.7234	0.0019	0.0255	9.84	90.91	91.44	0.1078	0.2955	0.1877	10.76	1.7858	0.1351	0.4306	0.0116
72	0.1466	0.7328	0.0019	0.0252	9.84	92.09	92.61	0.1065	0.2918	0.1853	10.62	1.7664	0.1323	0.4327	0.0116
73	0.1484	0.7422	0.0019	0.0250	9.84	93.27	93.78	0.1051	0.2881	0.1830	10.48	1.7476	0.1297	0.4347	0.0117
74	0.1503	0.7516	0.0019	0.0247	9.84	94.44	94.96	0.1038	0.2845	0.1807	10.35	1.7292	0.1270	0.4367	0.0117
75	0.1522	0.7609	0.0019	0.0245	9.84	95.62	96.13	0.1025	0.2810	0.1784	10.22	1.7113	0.1245	0.4385	0.0118
76	0.1541	0.7703	0.0019	0.0242	9.84	96.80	97.30	0.1013	0.2776	0.1762	10.10	1.6938	0.1220	0.4401	0.0119
77	0.1559	0.7797	0.0019	0.0239	9.84	97.98	98.47	0.1001	0.2742	0.1741	9.98	1.6767	0.1195	0.4417	0.0119
78	0.1578	0.7891	0.0019	0.0237	9.84	99.16	99.64	0.0989	0.2710	0.1720	9.86	1.6600	0.1171	0.4432	0.0120
79	0.1597	0.7984	0.0019	0.0234	9.84	100.33	100.82	0.0978	0.2678	0.1700	9.74	1.6438	0.1148	0.4446	0.0120
80	0.1616	0.8078	0.0019	0.0232	9.84	101.51	101.99	0.0966	0.2647	0.1680	9.63	1.6279	0.1126	0.4458	0.0120
81	0.1634	0.8172	0.0019	0.0229	9.84	102.69	103.16	0.0955	0.2616	0.1661	9.52	1.6124	0.1103	0.4470	0.0121
82	0.1653	0.8266	0.0019	0.0227	9.84	103.87	104.33	0.0945	0.2587	0.1642	9.41	1.5972	0.1082	0.4480	0.0121
83	0.1672	0.8359	0.0019	0.0224	9.84	105.05	105.51	0.0934	0.2558	0.1624	9.30	1.5824	0.1061	0.4489	0.0121
84	0.1691	0.8453	0.0019	0.0222	9.84	106.23	106.68	0.0924	0.2529	0.1606	9.20	1.5679	0.1040	0.4497	0.0122
85	0.1709	0.8547	0.0019	0.0219	9.84	107.40	107.85	0.0914	0.2502	0.1588	9.10	1.5537	0.1020	0.4504	0.0122
86	0.1728	0.8641	0.0019	0.0217	9.84	108.58	109.03	0.0904	0.2474	0.1571	9.00	1.5399	0.1000	0.4510	0.0122
87	0.1747	0.8734	0.0019	0.0214	9.84	109.76	110.20	0.0894	0.2448	0.1554	8.90	1.5263	0.0980	0.4515	0.0122
88	0.1766	0.8828	0.0019	0.0212	9.84	110.94	111.37	0.0885	0.2422	0.1537	8.81	1.5130	0.0961	0.4518	0.0122
89	0.1784	0.8922	0.0019	0.0209	9.84	112.12	112.55	0.0875	0.2396	0.1521	8.71	1.5000	0.0943	0.4520	0.0122
90	0.1803	0.9016	0.0019	0.0207	9.84	113.29	113.72	0.0866	0.2371	0.1505	8.62	1.4873	0.0925	0.4522	0.0122
91	0.1822	0.9109	0.0019	0.0204	9.84	114.47	114.89	0.0857	0.2347	0.1490	8.53	1.4748	0.0907	0.4521	0.0122
92	0.1841	0.9203	0.0019	0.0202	9.84	115.65	116.07	0.0849	0.2323	0.1474	8.45	1.4626	0.0889	0.4520	0.0122
93	0.1859	0.9297	0.0019	0.0199	9.84	116.83	117.24	0.0840	0.2300	0.1459	8.36	1.4507	0.0872	0.4518	0.0122
94	0.1878	0.9391	0.0019	0.0196	9.84	118.01	118.42	0.0832	0.2277	0.1445	8.28	1.4390	0.0856	0.4514	0.0122
95	0.1897	0.9484	0.0019	0.0194	9.84	119.18	119.59	0.0824	0.2254	0.1431	8.20	1.4275	0.0839	0.4509	0.0121
96	0.1916	0.9578	0.0019	0.0191	9.84	120.36	120.76	0.0816	0.2232	0.1416	8.12	1.4162	0.0823	0.4503	0.0121
97	0.1934	0.9672	0.0019	0.0189	9.84	121.54	121.94	0.0808	0.2211	0.1403	8.04	1.4052	0.0807	0.4496	0.0121
98	0.1953	0.9766	0.0019	0.0186	9.84	122.72	123.11	0.0800	0.2189	0.1389	7.96	1.3943	0.0792	0.4487	0.0121
99	0.1972	0.9859	0.0019	0.0184	9.84	123.90	124.29	0.0793	0.2169	0.1376	7.88	1.3837	0.0777	0.4478	0.0120
100	0.1991	0.9953	0.0019	0.0181	9.84	125.07	125.46	0.0785	0.2148	0.1363	7.81	1.3733	0.0762	0.4467	0.0120
													Total	24.2364	0.6048

Table B.1.: BEM without inflow factors, Take-off

Element	r [m]	$\frac{r}{R_d}$	dr [m]	c [m]	V_0 [m/s]	V_2 [m/s]	V_1 [m/s]	ϕ	θ	α	α°	C_l	C_d	ΔT	ΔQ
1	0.0134	0.0672	0.0019	0.0450	16.00	8.44	18.09	1.0852	1.1052	0.0200	1.15	0.4404	0.0571	0.0026	0.0001
2	0.0153	0.0766	0.0019	0.0429	16.00	9.62	18.67	1.0294	1.0394	0.0100	0.57	0.3602	0.0685	0.0022	0.0001
3	0.0172	0.0859	0.0019	0.0427	16.00	10.80	19.30	0.9771	0.9921	0.0150	0.86	0.4003	0.0628	0.0031	0.0001
4	0.0191	0.0953	0.0019	0.0424	16.00	11.98	19.99	0.9282	0.9432	0.0150	0.86	0.4003	0.0628	0.0037	0.0001
5	0.0209	0.1047	0.0019	0.0422	16.00	13.16	20.71	0.8827	0.8977	0.0150	0.86	0.4003	0.0628	0.0043	0.0002
6	0.0228	0.1141	0.0019	0.0419	16.00	14.33	21.48	0.8403	0.8603	0.0200	1.15	0.4404	0.0571	0.0056	0.0002
7	0.0247	0.1234	0.0019	0.0417	16.00	15.51	22.28	0.8009	0.8159	0.0150	0.86	0.4003	0.0628	0.0056	0.0002
8	0.0266	0.1328	0.0019	0.0414	16.00	16.69	23.12	0.7643	0.7793	0.0150	0.86	0.4003	0.0628	0.0062	0.0002
9	0.0284	0.1422	0.0019	0.0412	16.00	17.87	23.98	0.7303	0.7503	0.0200	1.15	0.4404	0.0571	0.0079	0.0003
10	0.0303	0.1516	0.0019	0.0409	16.00	19.05	24.87	0.6987	0.7137	0.0150	0.86	0.4003	0.0628	0.0077	0.0003
11	0.0322	0.1609	0.0019	0.0407	16.00	20.22	25.79	0.6693	0.6843	0.0150	0.86	0.4003	0.0628	0.0085	0.0003
12	0.0341	0.1703	0.0019	0.0404	16.00	21.40	26.72	0.6420	0.6620	0.0200	1.15	0.4404	0.0571	0.0106	0.0003
13	0.0359	0.1797	0.0019	0.0401	16.00	22.58	27.67	0.6165	0.6365	0.0200	1.15	0.4404	0.0571	0.0115	0.0004
14	0.0378	0.1891	0.0019	0.0399	16.00	23.76	28.64	0.5927	0.6127	0.0200	1.15	0.4404	0.0571	0.0125	0.0004
15	0.0397	0.1984	0.0019	0.0396	16.00	24.94	29.63	0.5705	0.5955	0.0250	1.43	0.4805	0.0514	0.0151	0.0005
16	0.0416	0.2078	0.0019	0.0394	16.00	26.11	30.63	0.5497	0.5697	0.0200	1.15	0.4404	0.0571	0.0147	0.0005
17	0.0434	0.2172	0.0019	0.0391	16.00	27.29	31.64	0.5302	0.5502	0.0200	1.15	0.4404	0.0571	0.0158	0.0005
18	0.0453	0.2266	0.0019	0.0389	16.00	28.47	32.66	0.5120	0.5370	0.0250	1.43	0.4805	0.0514	0.0188	0.0006
19	0.0472	0.2359	0.0019	0.0386	16.00	29.65	33.69	0.4949	0.5149	0.0200	1.15	0.4404	0.0571	0.0182	0.0006
20	0.0491	0.2453	0.0019	0.0384	16.00	30.83	34.73	0.4788	0.4988	0.0200	1.15	0.4404	0.0571	0.0194	0.0007
21	0.0509	0.2547	0.0019	0.0381	16.00	32.00	35.78	0.4636	0.4886	0.0250	1.43	0.4805	0.0514	0.0228	0.0007
22	0.0528	0.2641	0.0019	0.0379	16.00	33.18	36.84	0.4493	0.4843	0.0350	2.01	0.5607	0.0399	0.0288	0.0009
23	0.0547	0.2734	0.0019	0.0376	16.00	34.36	37.90	0.4358	0.4708	0.0350	2.01	0.5607	0.0399	0.0305	0.0009
24	0.0566	0.2828	0.0019	0.0374	16.00	35.54	38.97	0.4230	0.4630	0.0400	2.29	0.6009	0.0342	0.0348	0.0010
25	0.0584	0.2922	0.0019	0.0371	16.00	36.72	40.05	0.4109	0.4459	0.0350	2.01	0.5607	0.0399	0.0341	0.0010
26	0.0603	0.3016	0.0019	0.0369	16.00	37.90	41.13	0.3995	0.4345	0.0350	2.01	0.5607	0.0399	0.0359	0.0011
27	0.0622	0.3109	0.0019	0.0366	16.00	39.07	42.22	0.3887	0.4287	0.0400	2.29	0.6009	0.0342	0.0407	0.0012
28	0.0641	0.3203	0.0019	0.0364	16.00	40.25	43.32	0.3783	0.4133	0.0350	2.01	0.5607	0.0399	0.0397	0.0012
29	0.0659	0.3297	0.0019	0.0361	16.00	41.43	44.41	0.3685	0.4035	0.0350	2.01	0.5607	0.0399	0.0416	0.0013
30	0.0678	0.3391	0.0019	0.0358	16.00	42.61	45.51	0.3592	0.3992	0.0400	2.29	0.6009	0.0342	0.0469	0.0014
31	0.0697	0.3484	0.0019	0.0356	16.00	43.79	46.62	0.3503	0.3853	0.0350	2.01	0.5607	0.0399	0.0456	0.0014
32	0.0716	0.3578	0.0019	0.0353	16.00	44.96	47.73	0.3419	0.4019	0.0600	3.44	0.7613	0.0112	0.0660	0.0018
33	0.0734	0.3672	0.0019	0.0351	16.00	46.14	48.84	0.3338	0.3988	0.0650	3.72	0.8014	0.0055	0.0726	0.0019
34	0.0753	0.3766	0.0019	0.0348	16.00	47.32	49.95	0.3261	0.3861	0.0600	3.44	0.7613	0.0112	0.0716	0.0019
35	0.0772	0.3859	0.0019	0.0346	16.00	48.50	51.07	0.3187	0.3787	0.0600	3.44	0.7613	0.0112	0.0745	0.0020
36	0.0791	0.3953	0.0019	0.0343	16.00	49.68	52.19	0.3116	0.3766	0.0650	3.72	0.8014	0.0055	0.0817	0.0021
37	0.0809	0.4047	0.0019	0.0341	16.00	50.85	53.31	0.3048	0.3648	0.0600	3.44	0.7613	0.0112	0.0804	0.0022
38	0.0828	0.4141	0.0019	0.0338	16.00	52.03	54.44	0.2983	0.3583	0.0600	3.44	0.7613	0.0112	0.0834	0.0022
39	0.0847	0.4234	0.0019	0.0336	16.00	53.21	55.56	0.2921	0.3571	0.0650	3.72	0.8014	0.0055	0.0912	0.0024
40	0.0866	0.4328	0.0019	0.0333	16.00	54.39	56.69	0.2861	0.3461	0.0600	3.44	0.7613	0.0112	0.0894	0.0024
41	0.0884	0.4422	0.0019	0.0331	16.00	55.57	57.82	0.2804	0.3404	0.0600	3.44	0.7613	0.0112	0.0925	0.0025
42	0.0903	0.4516	0.0019	0.0328	16.00	56.75	58.96	0.2748	0.3398	0.0650	3.72	0.8014	0.0055	0.1008	0.0026
43	0.0922	0.4609	0.0019	0.0326	16.00	57.92	60.09	0.2695	0.3295	0.0600	3.44	0.7613	0.0112	0.0987	0.0027
44	0.0941	0.4703	0.0019	0.0323	16.00	59.10	61.23	0.2644	0.3244	0.0600	3.44	0.7613	0.0112	0.1018	0.0027
45	0.0959	0.4797	0.0019	0.0320	16.00	60.28	62.37	0.2594	0.3244	0.0650	3.72	0.8014	0.0055	0.1107	0.0029
46	0.0978	0.4891	0.0019	0.0318	16.00	61.46	63.51	0.2547	0.3147	0.0600	3.44	0.7613	0.0112	0.1081	0.0029
47	0.0997	0.4984	0.0019	0.0315	16.00	62.64	64.65	0.2501	0.3101	0.0600	3.44	0.7613	0.0112	0.1112	0.0030
48	0.1016	0.5078	0.0019	0.0313	16.00	63.81	65.79	0.2457	0.3107	0.0650	3.72	0.8014	0.0055	0.1207	0.0032
49	0.1034	0.5172	0.0019	0.0310	16.00	64.99	66.93	0.2414	0.3014	0.0600	3.44	0.7613	0.0112	0.1176	0.0032
50	0.1053	0.5266	0.0019	0.0308	16.00	66.17	68.08	0.2372	0.2972	0.0600	3.44	0.7613	0.0112	0.1208	0.0033
51	0.1072	0.5359	0.0019	0.0305	16.00	67.35	69.22	0.2332	0.2982	0.0650	3.72	0.8014	0.0055	0.1308	0.0034
52	0.1091	0.5453	0.0019	0.0303	16.00	68.53	70.37	0.2294	0.2894	0.0600	3.44	0.7613	0.0112	0.1272	0.0035
53	0.1109	0.5547	0.0019	0.0300	16.00	69.70	71.52	0.2256	0.2856	0.0600	3.44	0.7613	0.0112	0.1304	0.0035

Element	r [m]	$\frac{r}{R_d}$	dr [m]	c [m]	V_0 [m/s]	V_2 [m/s]	V_1 [m/s]	ϕ	θ	α	α°	C_l	C_d	ΔT	ΔQ
54	0.1128	0.5641	0.0019	0.0298	16.00	70.88	72.67	0.2220	0.2870	0.0650	3.72	0.8014	0.0055	0.1409	0.0037
55	0.1147	0.5734	0.0019	0.0295	16.00	72.06	73.82	0.2185	0.2785	0.0600	3.44	0.7613	0.0112	0.1368	0.0037
56	0.1166	0.5828	0.0019	0.0293	16.00	73.24	74.97	0.2151	0.2751	0.0600	3.44	0.7613	0.0112	0.1400	0.0038
57	0.1184	0.5922	0.0019	0.0290	16.00	74.42	76.12	0.2118	0.2768	0.0650	3.72	0.8014	0.0055	0.1510	0.0040
58	0.1203	0.6016	0.0019	0.0288	16.00	75.59	77.27	0.2086	0.2686	0.0600	3.44	0.7613	0.0112	0.1464	0.0040
59	0.1222	0.6109	0.0019	0.0285	16.00	76.77	78.42	0.2055	0.2655	0.0600	3.44	0.7613	0.0112	0.1496	0.0041
60	0.1241	0.6203	0.0019	0.0283	16.00	77.95	79.58	0.2024	0.2674	0.0650	3.72	0.8014	0.0055	0.1611	0.0042
61	0.1259	0.6297	0.0019	0.0280	16.00	79.13	80.73	0.1995	0.2595	0.0600	3.44	0.7613	0.0112	0.1559	0.0043
62	0.1278	0.6391	0.0019	0.0277	16.00	80.31	81.89	0.1967	0.2567	0.0600	3.44	0.7613	0.0112	0.1590	0.0044
63	0.1297	0.6484	0.0019	0.0275	16.00	81.49	83.04	0.1939	0.2589	0.0650	3.72	0.8014	0.0055	0.1710	0.0045
64	0.1316	0.6578	0.0019	0.0272	16.00	82.66	84.20	0.1912	0.2512	0.0600	3.44	0.7613	0.0112	0.1653	0.0045
65	0.1334	0.6672	0.0019	0.0270	16.00	83.84	85.35	0.1886	0.2486	0.0600	3.44	0.7613	0.0112	0.1684	0.0046
66	0.1353	0.6766	0.0019	0.0267	16.00	85.02	86.51	0.1860	0.2510	0.0650	3.72	0.8014	0.0055	0.1807	0.0048
67	0.1372	0.6859	0.0019	0.0265	16.00	86.20	87.67	0.1835	0.2435	0.0600	3.44	0.7613	0.0112	0.1745	0.0048
68	0.1391	0.6953	0.0019	0.0262	16.00	87.38	88.83	0.1811	0.2411	0.0600	3.44	0.7613	0.0112	0.1775	0.0049
69	0.1409	0.7047	0.0019	0.0260	16.00	88.55	89.99	0.1788	0.2838	0.1050	6.02	1.1222	0.0403	0.2650	0.0081
70	0.1428	0.7141	0.0019	0.0257	16.00	89.73	91.15	0.1765	0.2994	0.1230	7.05	1.2663	0.0609	0.3033	0.0099
71	0.1447	0.7234	0.0019	0.0255	16.00	90.91	92.31	0.1742	0.2955	0.1213	6.95	1.2532	0.0590	0.3050	0.0099
72	0.1466	0.7328	0.0019	0.0252	16.00	92.09	93.47	0.1720	0.2918	0.1197	6.86	1.2404	0.0572	0.3067	0.0100
73	0.1484	0.7422	0.0019	0.0250	16.00	93.27	94.63	0.1699	0.2881	0.1182	6.77	1.2279	0.0554	0.3083	0.0100
74	0.1503	0.7516	0.0019	0.0247	16.00	94.44	95.79	0.1678	0.2845	0.1167	6.68	1.2158	0.0537	0.3098	0.0100
75	0.1522	0.7609	0.0019	0.0245	16.00	95.62	96.95	0.1658	0.2810	0.1152	6.60	1.2039	0.0520	0.3112	0.0100
76	0.1541	0.7703	0.0019	0.0242	16.00	96.80	98.11	0.1638	0.2776	0.1137	6.52	1.1924	0.0503	0.3126	0.0101
77	0.1559	0.7797	0.0019	0.0239	16.00	97.98	99.28	0.1619	0.2742	0.1123	6.44	1.1812	0.0487	0.3139	0.0101
78	0.1578	0.7891	0.0019	0.0237	16.00	99.16	100.44	0.1600	0.2710	0.1110	6.36	1.1702	0.0472	0.3151	0.0101
79	0.1597	0.7984	0.0019	0.0234	16.00	100.33	101.60	0.1581	0.2678	0.1096	6.28	1.1595	0.0456	0.3162	0.0101
80	0.1616	0.8078	0.0019	0.0232	16.00	101.51	102.77	0.1563	0.2647	0.1083	6.21	1.1490	0.0441	0.3173	0.0101
81	0.1634	0.8172	0.0019	0.0229	16.00	102.69	103.93	0.1546	0.2616	0.1071	6.13	1.1388	0.0427	0.3183	0.0101
82	0.1653	0.8266	0.0019	0.0227	16.00	103.87	105.09	0.1528	0.2587	0.1058	6.06	1.1289	0.0413	0.3192	0.0101
83	0.1672	0.8359	0.0019	0.0224	16.00	105.05	106.26	0.1512	0.2558	0.1046	5.99	1.1191	0.0399	0.3200	0.0101
84	0.1691	0.8453	0.0019	0.0222	16.00	106.23	107.42	0.1495	0.2529	0.1034	5.93	1.1096	0.0385	0.3208	0.0101
85	0.1709	0.8547	0.0019	0.0219	16.00	107.40	108.59	0.1479	0.2502	0.1023	5.86	1.1003	0.0372	0.3215	0.0101
86	0.1728	0.8641	0.0019	0.0217	16.00	108.58	109.75	0.1463	0.2474	0.1011	5.79	1.0913	0.0359	0.3221	0.0101
87	0.1747	0.8734	0.0019	0.0214	16.00	109.76	110.92	0.1448	0.2448	0.1000	5.73	1.0824	0.0346	0.3226	0.0101
88	0.1766	0.8828	0.0019	0.0212	16.00	110.94	112.09	0.1432	0.2422	0.0989	5.67	1.0737	0.0334	0.3230	0.0100
89	0.1784	0.8922	0.0019	0.0209	16.00	112.12	113.25	0.1418	0.2396	0.0979	5.61	1.0652	0.0322	0.3234	0.0100
90	0.1803	0.9016	0.0019	0.0207	16.00	113.29	114.42	0.1403	0.2371	0.0968	5.55	1.0569	0.0310	0.3237	0.0100
91	0.1822	0.9109	0.0019	0.0204	16.00	114.47	115.58	0.1389	0.2347	0.0958	5.49	1.0487	0.0298	0.3239	0.0100
92	0.1841	0.9203	0.0019	0.0202	16.00	115.65	116.75	0.1375	0.2323	0.0948	5.43	1.0407	0.0287	0.3240	0.0099
93	0.1859	0.9297	0.0019	0.0199	16.00	116.83	117.92	0.1361	0.2300	0.0939	5.38	1.0329	0.0276	0.3240	0.0099
94	0.1878	0.9391	0.0019	0.0196	16.00	118.01	119.09	0.1348	0.2277	0.0929	5.32	1.0253	0.0265	0.3239	0.0099
95	0.1897	0.9484	0.0019	0.0194	16.00	119.18	120.25	0.1334	0.2254	0.0920	5.27	1.0178	0.0254	0.3238	0.0098
96	0.1916	0.9578	0.0019	0.0191	16.00	120.36	121.42	0.1322	0.2232	0.0911	5.22	1.0105	0.0244	0.3235	0.0098
97	0.1934	0.9672	0.0019	0.0189	16.00	121.54	122.59	0.1309	0.2211	0.0902	5.17	1.0033	0.0233	0.3232	0.0097
98	0.1953	0.9766	0.0019	0.0186	16.00	122.72	123.76	0.1296	0.2189	0.0893	5.12	0.9962	0.0223	0.3228	0.0097
99	0.1972	0.9859	0.0019	0.0184	16.00	123.90	124.93	0.1284	0.2169	0.0884	5.07	0.9893	0.0213	0.3223	0.0096
100	0.1991	0.9953	0.0019	0.0181	16.00	125.07	126.09	0.1272	0.2148	0.0876	5.02	0.9825	0.0204	0.3217	0.0095
													Total	15.2872	0.4584

Table B.2.: BEM without inflow factors, Cruise Flight

- For **take-off**, the total thrust and torque can be calculated, considering **two-blade propeller**:

$$T = 2 \cdot \Delta T = 48.5\ N$$

$$Q = 2 \cdot \Delta Q = 1.2\ N\ m$$

At this point, the thrust and torque coefficients can be calculated:

$$\begin{aligned} C_T &= \frac{T}{\rho n^2 {D_d}^4} = 0.1546 \\ C_Q &= \frac{Q}{\rho n^2 {D_d}^5} = 0.0096 \end{aligned} \tag{B.2.10}$$

Then, the propeller efficiency can be calculated:

$$\eta_{prop} = \frac{J\ C_T}{2\pi\ C_Q} \tag{B.2.11}$$

where the advance ratio is defined as:

$$J = \frac{u_\infty}{nD_d} = \frac{V_{T-O}}{nD_d} = 0.2460 \tag{B.2.12}$$

$$\eta_{prop_{T-O}} = \frac{J\ C_T}{2\pi\ C_Q} = 0.63$$

$$C_p = \frac{C_T \cdot J}{\eta_{prop}} = 0.0604$$

- The previous steps have been repeated for **cruise flight** conditions

$$T = 2 \cdot \Delta T = 30.6\ N$$

$$Q = 2 \cdot \Delta Q = 0.92\ N\ m$$

$$C_T = \frac{T}{\rho n^2 {D_d}^4} = 0.0985$$

$$C_Q = \frac{Q}{\rho n^2 {D_d}^5} = 0.0074$$

$$J_{cr} = \frac{V_{cr}}{nD_d} = 0.4$$

$$\eta_{prop_{cruise}} = \frac{J\ C_T}{2\pi\ C_Q} = 0.85$$

$$C_p = \frac{C_T \cdot J}{\eta_{prop}} = 0.0464$$

B.2.2 BEM with inflow factors

The complexity of the study begins when calculating the local angle of attack, which involves the flow components v_0 and v_2 at propeller disk.

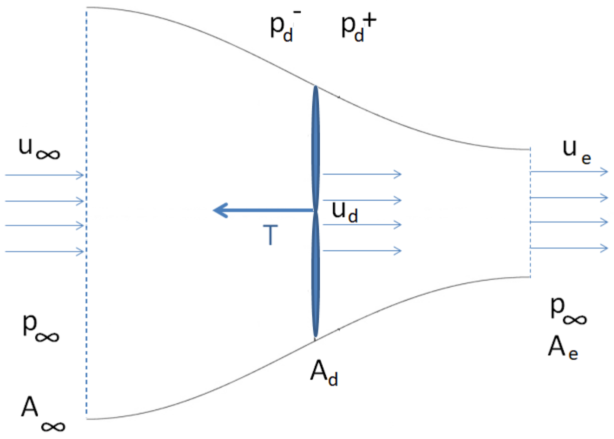

Figure B.3.: Streamtube diagram

From the Bernoulli equation and Conservation of momentum, the next equations can be found:

$$T = \rho A_d \cdot 2(u_e - u_\infty) = \pi {R_d}^2 \ \rho \ u_d(u_e - u_\infty) \tag{B.2.13}$$

which can be generalized for each blade element

$$\Delta T = \rho \ 2\pi r dr \ v_0(u_e - u_\infty) \tag{B.2.14}$$

and

$$u_d = v_0 = \frac{u_\infty + u_e}{2} \tag{B.2.15}$$

which can also be written as:

$$u_e = 2v_0 - u_\infty \tag{B.2.16}$$

For a streamtube, the axial flow and angular flow velocities can be considered of the form:

$$v_0 = u_\infty + a \cdot u_\infty \tag{B.2.17}$$

$$v_2 = \omega r - b \cdot \omega r \tag{B.2.18}$$

where **a** is the **axial inflow factor** and **b** is the **angular inflow factor**

Therefore, u_e can be rewritten as:

$$u_e = 2v_0 - u_\infty = u_\infty + 2a \cdot u_\infty = u_\infty(1 + 2a) \tag{B.2.19}$$

Therefore, the thrust and angular momentum equations for each blade element can be written as:

$$\Delta T = 2\pi r \ dr \ \rho \ u_\infty (1+a)(u_\infty (1+2a) - u_\infty) = 4\pi r \rho {u_\infty}^2 (1+a)a \ dr \tag{B.2.20}$$

and

$$\Delta Q = 2\pi r \rho u_\infty (1+a)(2b\omega r)r \ \ dr = 4\pi r^3 \rho \ u_\infty (1+a) b\omega \ dr \tag{B.2.21}$$

Summarizing all the previous steps and considering two-blade propeller, the next system of equations is obtained:

$$\begin{cases} \Delta T = \rho {v_1}^2 c(c_l \cos\phi - c_d \sin\phi)dr \\ \Delta Q = \rho {v_1}^2 c(c_d \cos\phi + c_l \sin\phi) r \cdot dr \\ v_1 = \sqrt{{v_0}^2 + {v_2}^2} \\ \alpha = \theta - \arctan\left(\dfrac{v_0}{v_2}\right) \\ \Delta T = 4\pi r \rho {u_\infty}^2 (1+a)a \ dr \\ \Delta Q = 4\pi r^3 \rho u_\infty (1+a) b\omega \ dr \end{cases} \tag{B.2.22}$$

The system can be resolved with an iterative method, supposing initial values for the inflow factors a and b. Then, through the [eq.41] and [eq.42] the velocity components v_0 and v_2 can be calculated. This will allow the calculation of v_1, and α. Then, ΔT and ΔQ can be calculated. To end the iterative process, [eq.44] and [eq.45] can be used to calculate more accurate values of the inflow factors **a** and **b**. The process should be repeated until the desired tolerance is achieved.

After the accurate inflow parameters are obtained, ΔT and ΔQ can be calculated, and then, the total thrust and torque can be obtained from the next equations:

$$\begin{gathered} T = \sum_{n=1}^{N} \Delta T \\ Q = \sum_{n=1}^{N} \Delta Q \end{gathered} \tag{B.2.23}$$

Then, thrust and torque coefficients can be found.

The twist distribution from the previous chapter will be used, since it provides reasonably acceptable angle of attack distribution for cruise flight and for take-off. The calculation is done by a script written in Python, following the next algorithm:

- introduction of twist (exponential function) and chord distribution (linear function)
- introduction of the number of blade elements

- introduction of initial inflow parameters **a** and **b**
- introduction of the advance speed, RPM and the desired tolerance

Step 1. Calculate v_0 and v_2 for each element

Step 2. Calculate v_1, ϕ and α for each element

Step 3. Calculate ΔT and ΔQ for each element

Step 4. Calculate **a** and **b** for each element using ΔT and ΔQ values

Step 5. Iterate the process until for each element the desired tolerance is met for **a** and **b**.

The script can be found attached in the "Extras" folder. At first, it has been used for cruise flight condition, where $u_\infty = 16\ [m/s]$, and it and has shown total convergence. The results are illustrated in the following figures.

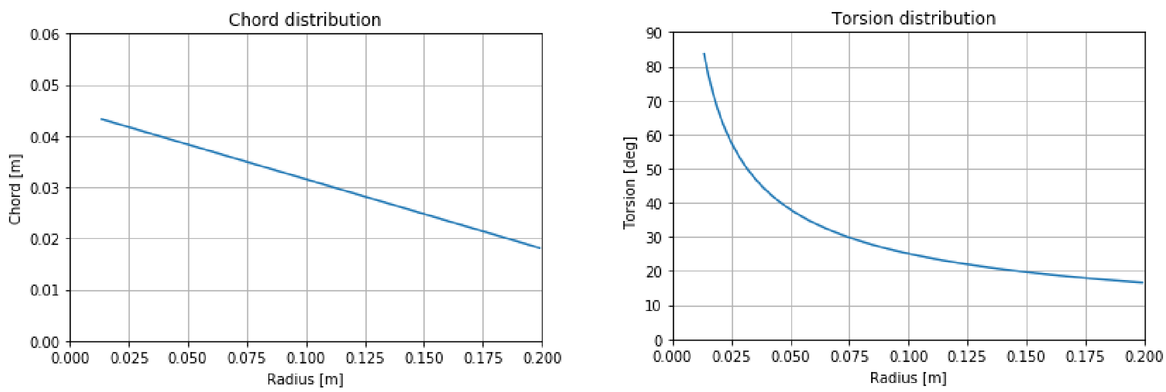

Figure B.4.: Propeller geometry: chord and twist distributions

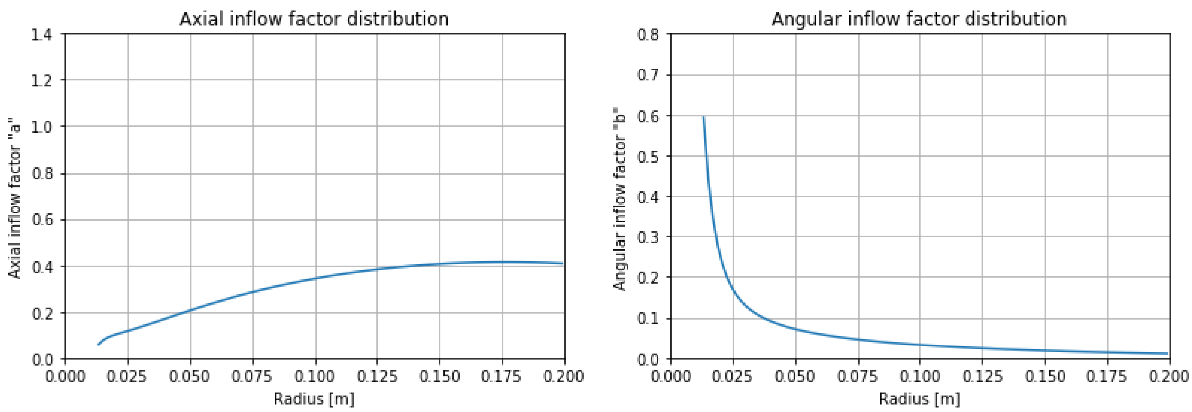

Figure B.5.: Inflow factors distribution for cruise flight

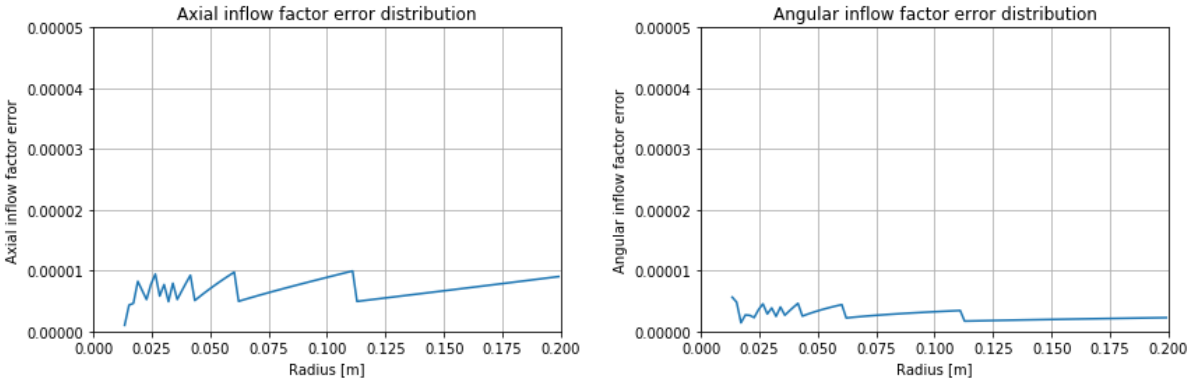

Figure B.6.: Inflow factors error distribution for cruise flight

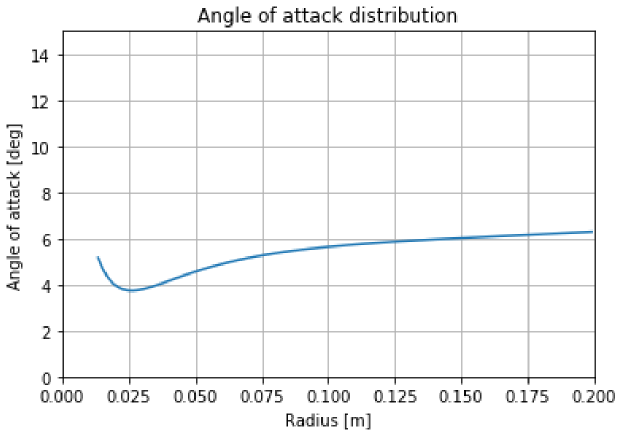

Figure B.7.: Angle of attack distribution for cruise flight

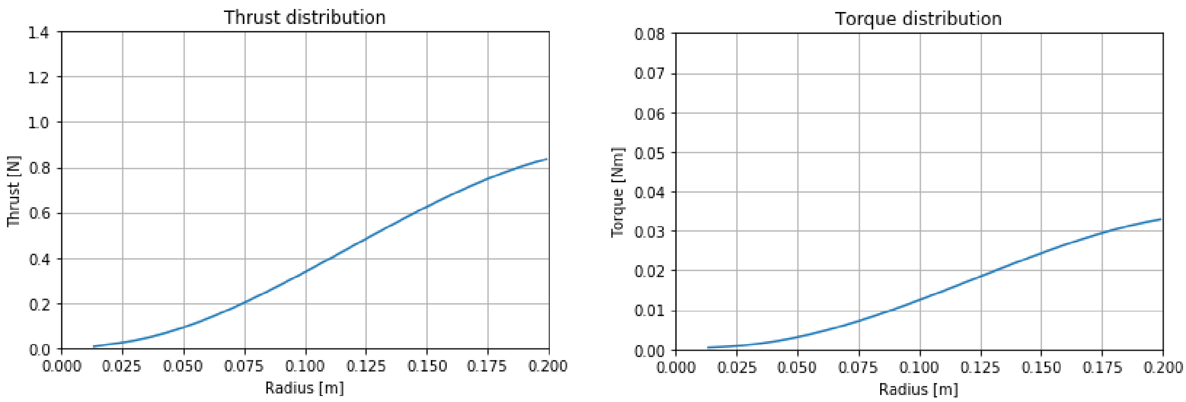

Figure B.8.: Thrust and torque distribution for cruise flight

The script also provided the next values for cruise flight:

- **Advance ratio:** $J \;=\; 0.4$
- **Thrust coefficient:** $C_t \;=\; 0.12530$
- **Torque coefficient:** $C_q \;=\; 0.01202$
- **Efficiency:** $\eta_p \;=\; 0.6634$
- **Power coefficient:** $C_p \;=\; 0.0756$

Then, the script has been used for the take-off condition, where u_∞ is considered to be 9.84 $[m/s]$, and it has also shown total convergence. The results are illustrated in the following figures.

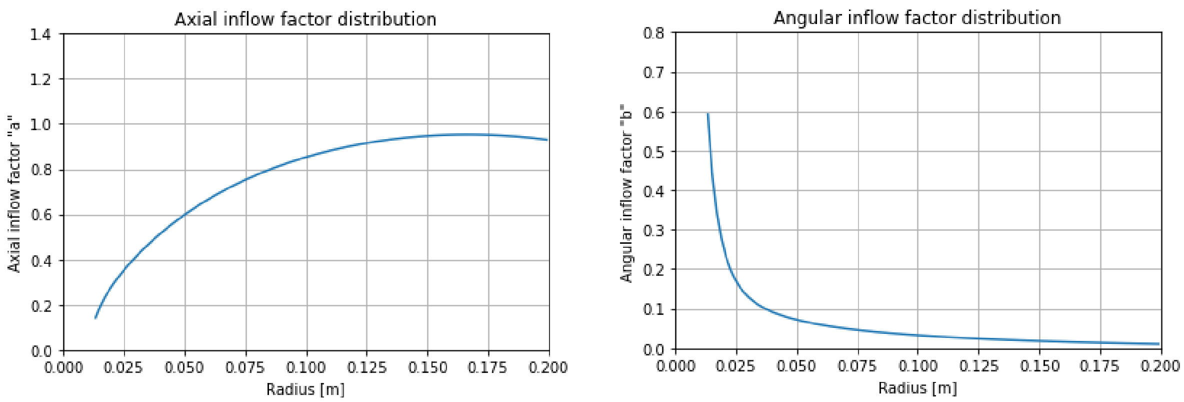

Figure B.9.: Inflow factors distribution for take-off

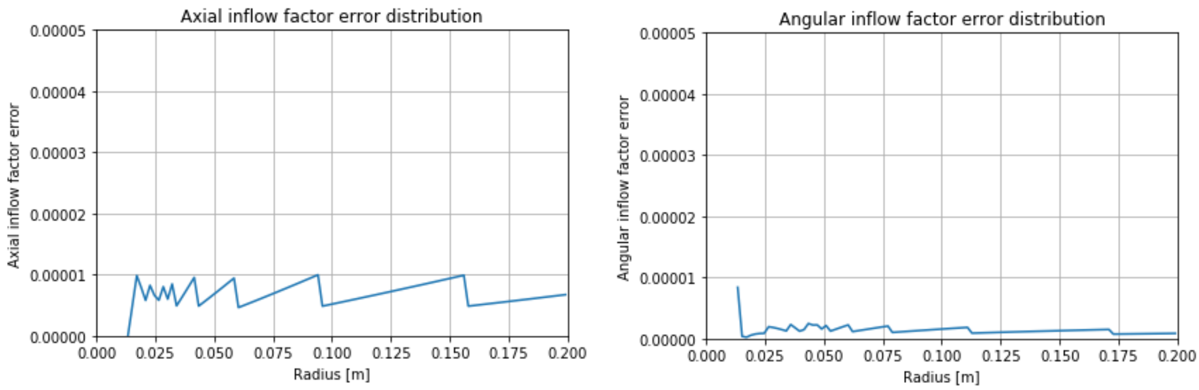

Figure B.10.: Inflow factors error distribution for take-off

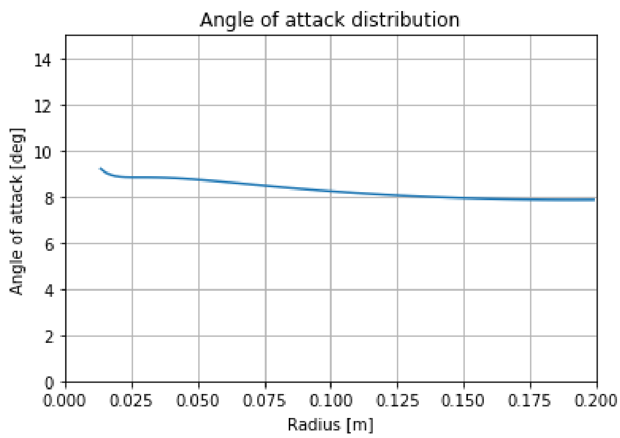

Figure B.11.: Angle of attack distribution for take-off

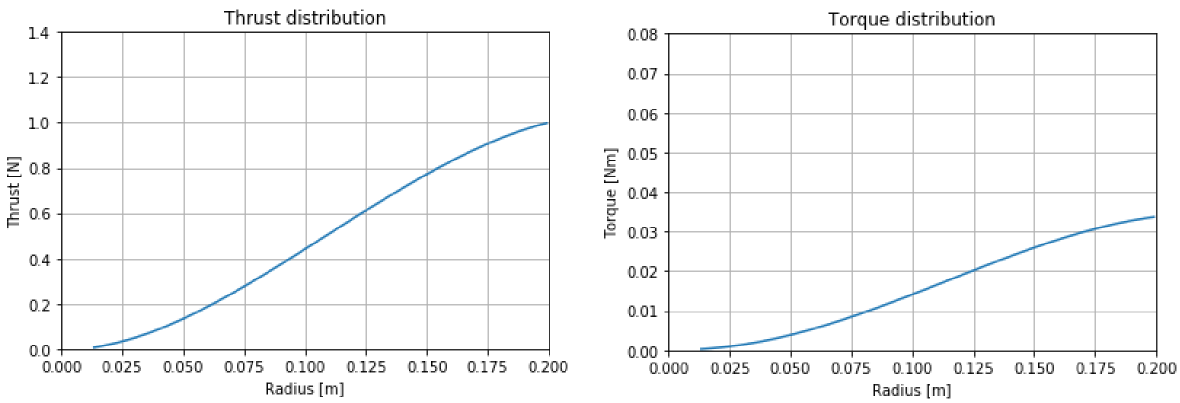

Figure B.12.: Thrust and torque distribution for take-off

The script also provided the next values, for take-off:

- **Advance ratio:** $J = 0.246$
- **Thrust coefficient:** $C_t = 0.15586$
- **Torque coefficient:** $C_q = 0.01284$
- **Efficiency:** $\eta_p = 0.4751$
- **Power coefficient:** $C_p = 0.0807$

The final conclusion is, that, the selected twist distribution provides almost constant angle of attack distribution, which is one of the design requirements. Also, it seems that the total thrust generated at take-off fulfills the requirement, which has been calculated in the previous chapter. At this point, since the propeller geometry has been defined, there are two ways to proceed for the propeller selection.

- The first option would be to create a prototype and analyze, experimentally, obtaining the efficiency and thrust coefficients.
- The second option, which is the one selected according to the project scope, consists of searching a similar model. Then, the experimental data will be obtained from the manufacturer.

B.2.3 BEM with inflow factors: Code

```
"""
BACHELOR OF SCIENCE THESIS
UNIVERSITAT POLITECNICA DE CATALUNYA
Bachelor's Degree In Aerospace Vehicle Engineering

Student: Armen Baghdasaryan
Director: Luis Manuel Perez Llera
Project:
Design of an Unmanned Aerial Vehicle with a Mass-Actuated Control System
--------------------------------------------------------------------------------
--- Blade Element Method with Inflow Factors : Propeller Design ----------------
--------------------------------------------------------------------------------
"""

import math
import matplotlib.pyplot as plt
a = float(input('Enter initial inflow factor A value: '))
b = float(input('Enter initial inflow factor B value: '))
radImput = float(input('Enter propeller Radius in meters: '))
n = int(input('Enter blade elements number: '))
epsilon = float(input('Enter desired tolerance: '))

omegaRPM = float(6000)
omegaRPS = float(omegaRPM/60)    #rev/s
omegaRADS = float((omegaRPM/60)*2*math.pi)   #rad/s
velAdv = float(9.84)
dr = (radImput-0.0125)/n
Rho = float(1.225)

#Propeller Geometry
rad_i = [1]*n
rad_i_dimless = [1]*n
chord = [1]*n
thetai = [1]*n
thetaDeg = [1]*n

#Inflow parameters
inflowAi = [1]*n
```

```
inflowBi = [1]*n
inflowAinew = [1]*n
inflowBinew = [1]*n
discriminflow = [1]*n

epsilonAi = [1]*n
epsilonBi = [1]*n
contador = [0]*n
velAxial = [1]*n
velTan = [1]*n
velTotal = [1]*n
phi = [1]*n

alpha = [1]*n
alphaDeg = [1]*n

CL = [1]*n
CD = [1]*n
clm = 0.16
clk = 0.3
cd_A = 0.000405555
cd_B = -0.00333333
cd_C = 0.025


incrTi = [1]*n
incrQi = [1]*n

#Geometry of each blade element
for i in range(n):
    rad_i[i] = 0.0125 + dr*(i + 0.5)          # element radial position
    rad_i_dimless[i] = rad_i[i] / radImput
    thetai[i] = 0.11*rad_i[i]**(-0.6)     # twist distribution
    thetaDeg[i] = thetai[i]*57.29578
    chord[i] = 0.0451 - 0.1356*rad_i[i]    # chord distribution


# Assign initial "a" and "b" inflow factors for each blade element
for i in range(n):
    inflowAi[i] = a
    inflowBi[i] = b
    inflowAinew[i] = a
```

```
    inflowBinew[i] = b

for i in range(n):
    while epsilonAi[i] > epsilon or epsilonBi[i] > epsilon :
        #S0 -------- initialize inflow factors
        inflowAi[i]=(inflowAinew[i] + inflowAi[i])/2
        inflowBi[i]=(inflowBinew[i] + inflowBi[i])/2

        #S1 -------- calculate velocity components according to inflow factors
        velAxial[i] = velAdv*(1 + inflowAi[i])
        velTan[i] = omegaRADS*rad_i[i]*(1 - inflowBi[i])

        #S2 -------- calculate alpha according to velocity components
        velTotal[i] = math.sqrt(velAxial[i]*velAxial[i] + velTan[i]*velTan[i])
        phi[i] = math.atan(( velAxial[i])/velTan[i])
        alpha[i] = thetai[i] - phi[i]
        alphaDeg[i] = alpha[i]*57.29578

        #S3 -------- calculate incrThrust and incrTorque
        CL[i] = clm*alphaDeg[i] + clk
        CD[i] = cd_A*alphaDeg[i]*alphaDeg[i] + cd_B*alphaDeg[i] + cd_C
        coeff = Rho*velTotal[i]*velTotal[i]*chord[i]*dr
        incrTi[i] = coeff*(CL[i]*math.cos(phi[i]) - CD[i]*math.sin(phi[i]))
        incrQi[i] = coeff
                    *rad_i[i]*(CD[i]*math.cos(phi[i]) + CL[i]*math.sin(phi[i]))

        #S4 -------- calculate inflow factors A and B
        discriminflow[i] =
            abs(1 + ((incrTi[i])/(Rho*math.pi*rad_i[i]*dr*velAdv*velAdv)))

        #solution of eq a^2+a+k=0
        inflowAinew[i] = float((math.sqrt(discriminflow[i]) - 1)/2)
        inflowBinew[i] = float((incrQi[i])/(4*math.pi*rad_i[i]*rad_i[i]*rad_i[i]
                        *Rho*velAdv*(1 + inflowAinew[i])*omegaRADS*dr))
        epsilonAi[i] = abs(inflowAinew[i] - inflowAi[i])
        epsilonBi[i] = abs(inflowBinew[i] - inflowBi[i])
        contador[i] += 1


plt.xlabel('Radius [m]')
plt.ylabel('Chord [m]')
plt.title('Chord distribution')
```

```
plt.plot(rad_i, chord)
plt.axis([0, 0.2, 0, 0.06])
plt.grid()
plt.show()

plt.xlabel('Radius [m]')
plt.ylabel('Thorsion [deg]')
plt.title('Thorsion distribution')
plt.plot(rad_i, thetaDeg)
plt.axis([0, 0.2, 0, 90])
plt.grid()
plt.show()

plt.xlabel('Radius [m]')
plt.ylabel('Angle of attack [deg]')
plt.title('Angle of attack distribution')
plt.plot(rad_i, alphaDeg)
plt.axis([0, 0.2, 0, 15])
plt.grid()
plt.show()


plt.xlabel('Radius [m]')
plt.ylabel('Axial inflow factor error')
plt.title('Axial inflow factor error distribution')
plt.plot(rad_i, epsilonAi)
plt.axis([0, 0.2, 0, 0.00005])
plt.grid()
plt.show()

plt.xlabel('Radius [m]')
plt.ylabel('Angular inflow factor error')
plt.title('Angular inflow factor error distribution')
plt.plot(rad_i, epsilonBi)
plt.axis([0, 0.2, 0, 0.00005])
plt.grid()
plt.show()

plt.xlabel('Radius [m]')
plt.ylabel('Axial inflow factor "a"')
plt.title('Axial inflow factor distribution')
plt.plot(rad_i, inflowAinew)
```

```
plt.axis([0, 0.2, 0, 1.4])
plt.grid()
plt.show()

plt.xlabel('Radius [m]')
plt.ylabel('Angular inflow factor "b"')
plt.title('Angular inflow factor distribution')
plt.plot(rad_i, inflowBinew)
plt.axis([0, 0.2, 0, 0.8])
plt.grid()
plt.show()

plt.xlabel('Radius [m]')
plt.ylabel('Thrust [N]')
plt.title('Thrust distribution')
plt.plot(rad_i, incrTi)
plt.axis([0, 0.2, 0, 1.4])
plt.grid()
plt.show()

plt.xlabel('Radius [m]')
plt.ylabel('Torque [Nm]')
plt.title('Torque distribution')
plt.plot(rad_i, incrQi)
plt.axis([0, 0.2, 0, 0.08])
plt.grid()
plt.show()

vartotalT = sum(incrTi)
vartotalQ = sum(incrQi)
varJ = float(velAdv/(omegaRPS*2*radImput))
varCt = float(vartotalT/(Rho*omegaRPS*omegaRPS*(2*radImput)**4))
varCq = float(vartotalQ/(Rho*omegaRPS*omegaRPS*(2*radImput)**5))
varEff = float(varJ*varCt/(2*math.pi*varCq))
varCp = float(varJ*varCt/(varEff))

print('Advance ratio J', varJ,)
print('Thrust coefficient  Ct', varCt,)
print('Torque coefficient  Cq', varCq,)
print('Efficiency ', varEff,)
print('Power coefficient Cp', varCp,)
```

Part C

SYSTEMS

Introduction

Since one of the main features of the designed vehicle is mapping, a list of some optional cameras and thermal sensors under 250 grams is included.

Optional cameras and sensors

C.2.1 HD cameras

- **Sony FCB-H11**

  A very popular product due to its small form factor, weight and great image quality. According to the manufacturer, it extends application possibilities by incorporating a new Day/Night function that enables the camera to capture high-quality color images during the day. Also, it has a Picture Freeze Function which enables to capture a still image while the camera is panning, tilting, zooming, focusing, initializing the lens, or performing preset operations. Some of the specifications are listed below:

Figure C.1.: Sony FCB-H11 HD Camera [35]

Parameter	**Value**
Weight	120 g
Width	47 mm
Height	43 mm
Lens Diameter	27 mm
Aperture Control	16 steps
Camera Operation Switch	Zoom TELE/ Zoom WIDE
Focusing System	Auto Focus Mode, Manual Focus Mode
Electronic Shutter Speed	1 ms
Lens	x 10 Zoom
Sensor Type	1/3 type CMOS
Signal System	HD: 1080i/59.94

Table C.1.: Sony FCB-H11 Specifications [35]

- **Sony FCB-EX1020**

  Described by the manufacturer as a color block camera which offers excellent picture quality, superb flexibility, and easy operation in a variety of applications ranging from surveillance to traffic monitoring. In Progressive Scan mode, the video signal is processed by progressive scan to achieve clear images without any flickering effect. The camera has high sensitivity, which is enough for use in video security. It also offers an enhanced noise reduction and color enhancement.

Figure C.2.: Sony FCB-EX1020 HD Camera [35]

Parameter	Value
Weight	230 g
Width	50 mm
Height	57 mm
Lens Diameter	38 mm
Aperture Control	16 steps
Camera Operation Switch	Zoom TELE/ Zoom WIDE
Focusing System	Auto Focus, Infinity Mode, Manual Mode
Electronic Shutter Speed	1 ms
Lens	x 36 Zoom
Sensor Type	1/4 type PS CCD
Signal System	PAL (Interlaced-PsF mode)

Table C.2.: Sony FCB-EX1020 Specifications [35]

- **Panasonic GP-MH310**

  Described by the manufacturer as a Single Chip Full HD Module Camera, it outstanding HD resolution and superior color performance at the right price, and the right size for a wide variety of medical and industrial applications. With outstanding performance, the camera delivers native 1080p/60p resolution, plus multi-format capability in a compact and lightweight camera module.

Figure C.3.: Panasonic GP-MH310 HD Camera [36]

Parameter	Value
Weight	180 g
Width	43.7 mm
Height	44.2 mm
Lens Diameter	33 mm
Aperture Control	16 steps
Camera Operation Switch	Zoom TELE/ Zoom WIDE
Focusing System	Auto Focus, Infinity Mode, Manual Mode
Electronic Shutter Speed	1 ms
Lens	x 16 Zoom
Sensor Type	1/2.5 type MOS
Signal System	NTSC / PAL

Table C.3.: Panasonic GP-MH310 Specifications [36]

- **Hitachi DI-SC120R**

  According to the manufacturer, the DI-SC120R is a compact chassis-type camera delivering unparalleled low light performance for video applications seeking HD digital video output. The 1/3-inch color CCD sensor makes it suitable for surveillance, traffic, low vision, in car video or telepresence applications.

Figure C.4.: Hitachi DI-SC120R HD Camera [37]

Parameter	**Value**
Weight	240 g
Width	50 mm
Height	60 mm
Lens Diameter	43 mm
Aperture Control	20 steps
Camera Operation Switch	Zoom TELE/ Zoom WIDE
Focusing System	Auto Focus, Infinity Mode, Manual Mode
Electronic Shutter Speed	1 ms
Lens	x 30 Zoom
Sensor Type	1/3 type
Signal System	YUV422

Table C.4.: Hitachi DI-SC120R Specifications [37]

C.2.2 Thermal sensors

- **FLIR Tau 2**

According to the manufacturers description, FLIR Tau 2 is a family of longwave thermal imaging cameras, with unmatched set of features, making them well-suited for demanding applications, such as unmanned vehicles (UVs), thermal weapon sights, and handheld imagers. Improved electronics now give Tau 2 even more capabilities, including radiometry, increased sensitivity, a 60Hz frame rate, and powerful image processing modes that dramatically improve detail and contrast.

Figure C.5.: FLIR Tau 2 thermal sensor [38]

Parameter	Value
Weight	71 g - 200 g
Width	19 mm - 62 mm
Height	19 mm - 62 mm
Lens Diameter	29 mm - 61 mm
Focal ratio	f/1.0
Spectral Band	7.5 - 13.5 μm
Pixel Pitch	17 μm
Zoom Type	Digital
System Type	Longwave Infrared
Analog Video	NTSC / PAL
Analog Video Frame rate	30/60 Hz
Digital Video	8-bit / 14-bit LVDS/ CMOS

Table C.5.: FLIR Tau 2 Specifications [38]

- **FLIR Tau SWIR**

  FLIR Tau SWIR is a size, weight and power optimized termal sensor camera. Described by the manufacturer as a short-wave infrared camera, it is designed for a variety of OEM applications, including hyperspectral instrumentation, electrooptical payloads, counterfeit detection, and portable applications. The Tau SWIR provides outstanding image quality and performance over a wide range of imaging and light level conditions. Tau SWIR incorporates the FLIR high resolution 640 x 512 ISC1202 Indium Gallium Arsenide (InGaAs) 15-micron pitch focal plane array (FPA) and includes several advanced camera controls features.

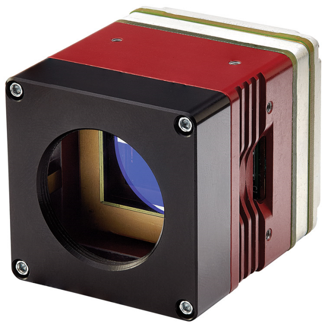

Figure C.6.: FLIR Tau SWIR thermal sensor [38]

Parameter	Value
Weight	81 g
Width	38 mm
Height	38 mm
Lens Diameter	25 mm
Focal ratio	f/1.0
Spectral Band	0.7 - 1.7 μm
Pixel Pitch	15 μm
Zoom Type	Digital
System Type	Shortwave Infrared
Analog Video	NTSC / PAL
Analog Video Frequency	60/120 Hz
Digital Video	14-bit CMOS

Table C.6.: FLIR Tau SWIR Specifications [38]

- **NanoCore 640M 5000978-3**

  A small size, light weight, and low power thermal sensor, which offers two channels of digital video operating simultaneously. Also, according to the manufacturer, it includes electronics for the control off video formats and input power.

Figure C.7.: NanoCore 640M 5000978-2 thermal sensor [41]

Parameter	**Value**
Weight	233 g
Width	55 mm
Height	55 mm
Lens Diameter	60 mm
Focal ratio	f/1.2
Spectral Band	8 - 14 μm
Pixel Pitch	17 μm
Zoom Type	Digital
System Type	Longwave Infrared
Analog Video	NTSC
Analog Video Frequency	30 Hz
Digital Video	8/16/24-bit CameraLink

Table C.7.: NanoCore 640 M Specifications [41]

- **DRS Tamarisk 640**

  The Tamarisk 640 provides high performance while maintaining a small size, low weight, and minimal power consumption. It uses uncooled, highly sensitive Vanadium Oxide detector, incorporating patented absorber technology to capture infrared energy in the 8 to 14 μm spectrum. This high-performance core is enhanced with dynamic range, pixel saturation logic, multi-mode Image Contrast Enhancement and 24-bit RGB color.

Figure C.8.: DRS Tamarisk 640 thermal sensor [39]

Parameter	**Value**
Weight	230 g
Width	50 mm
Height	47 mm
Lens Diameter	35 mm
Focal ratio	f/1.2
Spectral Band	8 - 14 μm
Pixel Pitch	17 μm
Zoom Type	Digital
System Type	Longwave Infrared
Analog Video	NTSC / PAL
Analog Video Frequency	25/30 Hz
Digital Video	14-bit / 8-bit LVCMOS

Table C.8.: DRS Tamarisk 640 Specifications [39]

Part D

PERFORMANCE AND FLIGHT MECHANICS

Introduction

The aim of this chapter is to explain the methodology followed to populate the inertia tensor variation spreadsheets. As explained in the project Report, each component of the inertia matrix has been calculated based on this data. Additionally, the flight control algorithm code has been provided, which has been used for the simulation.

D.1.1 Inertia Tensor Variation

The objective has been to determine the inertia matrix variation as a function of the center of gravity location.

$$I_i = f_i(x_s, y_s)$$

where x_s and y_s are the coordinates of the center of gravity.
The following steps have been applied:

- Prepare the CAD prototype, including weight distribution.
- Create a new table for each X_{CG}, where $X_{CG1} = 0.390m$, $X_{CG2} = 0.395m$, $X_{CG3} = 0.400m$, $X_{CG4} = 0.405m$, $X_{CG5} = 0.410m$.
- For each X_{CG} populate the tables with inertia measurements provided by CATIA V5, changing the Y_{CG}.

Then, the following five tables have been obtained. As explained in the project Report, each component of the Inertia matrix has been analyzed individually.

$X_{CG} = 0.390m$						
Y_{CG}	I_x	I_y	I_z	I_{xy}	I_{xz}	I_{yz}
0.000	0.354	0.151	0.498	0	-0.023	0
0.015	0.355	0.151	0.499	8.61E-04	-0.023	1.14E-04
0.030	0.36	0.151	0.504	0.0015	-0.023	2.28E-04
0.045	0.368	0.151	0.512	0.0025	-0.023	3.43E-04
0.060	0.378	0.151	0.522	0.003	-0.023	4.57E-04
0.075	0.392	0.151	0.536	0.004	-0.023	5.72E-04
0.090	0.409	0.151	0.553	0.005	-0.023	6.86E-04
0.105	0.429	0.151	0.573	0.006	-0.023	8.01E-04
0.120	0.451	0.151	0.595	0.007	-0.023	9.15E-04
0.141	0.481	0.151	0.625	0.008	-0.023	0.001

Table D.1.: I vs Y_{CG} at $X_{CG} = 0.390m$

$X_{CG} = 0.395m$						
Y_{CG}	I_x	I_y	I_z	I_{xy}	I_{xz}	I_{yz}
0.000	0.354	0.139	0.486	0	-0.021	0
0.015	0.355	0.139	0.487	0.001	-0.021	1.58E-04
0.030	0.36	0.139	0.492	0.002	-0.021	3.16E-04
0.045	0.368	0.139	0.5	0.003	-0.021	4.76E-04
0.060	0.378	0.139	0.51	0.005	-0.021	6.33E-04
0.075	0.392	0.139	0.524	0.006	-0.021	7.91E-04
0.090	0.409	0.139	0.541	0.007	-0.021	9.50E-04
0.105	0.429	0.139	0.561	0.008	-0.021	0.0011
0.120	0.451	0.139	0.584	0.009	-0.021	0.0012
0.141	0.481	0.139	0.613	0.011	-0.021	0.0013

Table D.2.: I vs Y_{CG} at $X_{CG} = 0.395m$

$X_{CG} = 0.400m$						
Y_{CG}	I_x	I_y	I_z	I_{xy}	I_{xz}	I_{yz}
0.000	0.354	0.128	0.476	0	-0.019	0
0.015	0.355	0.128	0.477	0.001	-0.019	2.02E-04
0.030	0.36	0.128	0.482	0.003	-0.019	4.04E-04
0.045	0.368	0.128	0.489	0.004	-0.019	6.06E-04
0.060	0.378	0.128	0.5	0.006	-0.019	8.09E-04
0.075	0.392	0.128	0.514	0.007	-0.019	0.001
0.090	0.409	0.128	0.53	0.009	-0.019	0.0013
0.105	0.429	0.128	0.55	0.01	-0.019	0.0016
0.120	0.451	0.128	0.573	0.012	-0.019	0.0019
0.141	0.481	0.128	0.603	0.013	-0.019	0.0022

Table D.3.: I vs Y_{CG} at $X_{CG} = 0.400m$

$X_{CG} = 0.405m$						
Y_{CG}	I_x	I_y	I_z	I_{xy}	I_{xz}	I_{yz}
0.000	0.354	0.119	0.467	0	-0.018	0
0.015	0.355	0.119	0.468	0.0018	-0.018	2.46E-04
0.030	0.36	0.119	0.473	0.0034	-0.018	4.92E-04
0.045	0.368	0.119	0.48	0.005	-0.018	7.38E-04
0.060	0.378	0.119	0.491	0.007	-0.018	9.84E-04
0.075	0.392	0.119	0.505	0.009	-0.018	0.0012
0.090	0.409	0.119	0.522	0.01	-0.018	0.0015
0.105	0.429	0.119	0.541	0.012	-0.018	0.0018
0.120	0.451	0.119	0.564	0.014	-0.018	0.0022
0.141	0.481	0.119	0.594	0.016	-0.018	0.0025

Table D.4.: I vs Y_{CG} at $X_{CG} = 0.405m$

$X_{CG} = 0.410m$						
Y_{CG}	I_x	I_y	I_z	I_{xy}	I_{xz}	I_{yz}
0.000	0.354	0.111	0.459	0	-0.017	0
0.015	0.355	0.111	0.46	0.002	-0.017	2.94E-04
0.030	0.36	0.111	0.465	0.004	-0.017	5.88E-04
0.045	0.368	0.111	0.472	0.006	-0.017	8.82E-04
0.060	0.378	0.111	0.483	0.008	-0.017	0.0011
0.075	0.392	0.111	0.497	0.01	-0.017	0.0013
0.090	0.409	0.111	0.514	0.012	-0.017	0.0017
0.105	0.429	0.111	0.534	0.014	-0.017	0.002
0.120	0.451	0.111	0.556	0.016	-0.017	0.0024
0.141	0.481	0.111	0.586	0.019	-0.017	0.0027

Table D.5.: I vs Y_{CG} at $X_{CG} = 0.410m$

D.1.2 Conclusion

Throughout this chapter, different analysis have been done, and it is reasonable to summarize all the results together:

- Longitudinal stability control system

$$\begin{cases} \delta_x(t) = 0.09 \cdot t + 0.29 \\ 0.0m < \delta_x < 0.180m \\ X_{CG} = x_s = 390.3 + 0.1125 \cdot \delta_x \\ 0.390m < x_s < 0.410m \\ M\Big|_{X_{CG}=x_s} = \dfrac{\rho u_\infty^2 S\bar{c}}{2}\Big((0.4796 \cdot x_s - 0.1963)\boldsymbol{\alpha} + (-0.3846 \cdot x_s + 0.1814)\Big) \end{cases}$$

- Lateral stability control system

$$\begin{cases} \delta_{y_{max}} = \pm 0.2(t - t_{acc}) \\ -0.365m < \delta_y < 0.365m \\ Y_{CG} = y_s = 0.3865 \cdot \delta_y \\ -0.141m < y_s < 0.141m \\ \Delta L\Big|_{Y_{CG}=y_s} = \dfrac{\rho S u_\infty^2}{2b}(4.76\alpha + 0.0189) \cdot 1.2856 y_s \end{cases}$$

- Inertia tensor components variation

$$\begin{cases} I_x = 5.9826 \cdot y_s^2 + 0.0819 \cdot y_s + 0.3528 \\ I_y = 28.571 \cdot x_s^2 - 24.857 \cdot x_s + 5.4996 \\ I_z = -1.904 \cdot x_s + 6.924 \cdot y_s^2 + 0.0204 \cdot y_s + 1.2716 \\ I_{xy} = \big(3.828 \cdot x_s - 1.4335\big) \cdot y_s \\ I_{xz} = -8.5714 \cdot x_s^2 + 7.1571 \cdot x_s - 1.5106 \\ I_{yz} = \big(- 2066.7 \cdot x_s^3 + 2464.6 \cdot x_s^2 - 978.85 \cdot x + 129.49\big) \cdot y_s \end{cases}$$

Flight Control Algorithm: Code

```python
"""
BACHELOR OF SCIENCE THESIS
UNIVERSITAT POLITECNICA DE CATALUNYA
Bachelor's Degree In Aerospace Vehicle Engineering

Student: Armen Baghdasaryan
Director: Luis Manuel Perez Llera
Project:
Design of an Unmanned Aerial Vehicle with a Mass-Actuated Control System
--------------------------------------------------------------------------------
--- Flight Control Algorithm and Simulations -----------------------------------
--------------------------------------------------------------------------------
"""

import numpy as np
import math
import matplotlib.pyplot as plt

dt = 0.05
grav = 9.81
rho = 1.225

mass = 4

wingArea = 1.05
meanChord = 0.51
alphaCruise = 2.6
alphaStall = 15
velCruise = 16
velGustCruise = 15.7
iterations = list(range(12000))
time = []
alpha = []
alphaTrue = []

velHor = []
velVer = []
velAng = []

```

```
velHorWind = []
velVerWind = []

XCG = []
LIFT = []
WEIGHT = []

accHor = []
accVer = []
accAng = []

height = []

windVerticalSpeed = []
windHorizontalSpeed = []
for i in iterations:
    time.append(dt*i)
    WEIGHT.append(mass*grav)

for i in time:
    if (i >=50 and i < 120):
        windVerticalSpeed.append(velGustCruise)
    else:
        windVerticalSpeed.append(0)

    windHorizontalSpeed.append(0)

# ----------  functions  ---------------------------------------------------
def calculateAlpha(alpha_init, vel_ang_init, acc_ang_init, dt):
    alpha_end = alpha_init + vel_ang_init*dt + 0.5*acc_ang_init*dt*dt
    return alpha_end


def calculateSpeedHor(vel_hor_init, acc_hor, dt):
    vel_hor_end = vel_hor_init + acc_hor*dt
    return vel_hor_end

def calculateSpeedVert(vel_ver_init, acc_ver, dt):
    vel_vert_end = vel_ver_init + acc_ver*dt
    return vel_vert_end

def calculateSpeedAng(vel_ang_init, acc_ang, dt):
```

```
    vel_ang_end = vel_ang_init + acc_ang*dt
    return vel_ang_end

def sumaF_hor(drag, thrust, mass):
    acc_hor = (thrust - drag)/mass
    return acc_hor

def sumaF_ver(lift, weight, mass):
    acc_ver = (lift - weight)/mass
    return acc_ver

def sumaMpitch(alphaDegrees, xcg, dynPress):
    alphaLocal = alphaDegrees
    if (alphaDegrees > 15):
            alphaLocal = 15
    moment = dynPress * wingArea * meanChord
            * ((0.48 * xcg - 0.20)*alphaLocal + (-0.39 * xcg + 0.20))

    Iyy = 28.60 * xcg * xcg + 24.90 * xcg + 5.50
    alpha_dot_dot = moment / Iyy
    return alpha_dot_dot

def calculateLiftCoef(alphaDegrees):
    if (alphaDegrees > alphaStall or alphaDegrees < -8):
        return 0 #stall
    else:
        alphaRad = math.radians(alphaDegrees)
        cl = 4.76*alphaRad + 0.018
        return cl


def calculateDragCoef(alphaDegrees):
    cd = 0.0004*alphaDegrees*alphaDegrees - 0.003*alphaDegrees + 0.025
    return cd

def pushThrottle(alphaDegrees):
    if (alphaDegrees < alphaCruise):
        horSpeedConstant = 1
    elif(alphaDegrees > alphaStall):
        horSpeedConstant = 1
    else:
        horSpeedConstant = 1
```

```
    return horSpeedConstant

# ----------  Controller functions ----------------------------------------------
def moveXCG(alphaDegrees):
    if (alphaDegrees < alphaCruise):
        xcg = 0.410
    elif(alphaDegrees > alphaStall):
        xcg = 0.390
    else:
        xcg = 0.400
    return xcg


# ----------  t0  pre-definition -----------------------------------------------
alpha.append(alphaCruise)
alphaTrue.append(alphaCruise)

velHor.append(velCruise)
velVer.append(0)
velAng.append(0)

accHor.append(0)
accVer.append(0)
accAng.append(0)

height.append(150)
XCG.append(0.40)
LIFT.append(mass*grav)
# ----------  t[i] routine  -----------------------------------------------------
# Get previous step alpha, speeds, accelerations
# Calculate this state alpha and speeds due to time step (integration)
# Calculate this state accelerations (equilibrium)
# Append to global lists
for i in range(1, len(time)):
    print("........................... t  =   ", i, '  .....................')
    alpha_prev = alpha[i-1]

    vel_ang_prev = velAng[i-1]
    vel_hor_prev = velHor[i-1]
    vel_vert_prev = velVer[i-1]

    acc_hor_prev = accHor[i-1]
```

```
    acc_ver_prev = accVer[i-1]
    acc_ang_prev = accAng[i-1]

    vel_hor_this = calculateSpeedHor(vel_hor_prev, acc_hor_prev, dt)
    vel_vert_this = calculateSpeedVert(vel_vert_prev, acc_ver_prev, dt)
    vel_ang_this = calculateSpeedAng(vel_ang_prev, acc_ang_prev, dt)
    alpha_this = calculateAlpha(alpha_prev, vel_ang_prev, acc_ang_prev, dt)


    relVelHorizontal = windHorizontalSpeed[i]-vel_hor_this
    relVelVertical = windVerticalSpeed[i] - vel_vert_this
    trueAirSpeed = math.sqrt(
            relVelHorizontal*relVelHorizontal + relVelVertical*relVelVertical)

    dynamicPressure = 0.5 * rho * trueAirSpeed * trueAirSpeed

    alpha_gust_this = math.atan(-relVelVertical/relVelHorizontal)
    alpha_gust_this = math.degrees(alpha_gust_this)

    alpha_this_true = alpha_this + 1*alpha_gust_this
    # print(alpha_this, 'to.....raddd ....', alpha_this_true)

    coefLift = calculateLiftCoef(alpha_this_true)
    coefDrag = calculateDragCoef(alpha_this_true)
    Lift = coefLift * dynamicPressure * wingArea
    Drag = coefDrag * dynamicPressure * wingArea
    horSpeedConstant = pushThrottle(alpha_this_true)
    Thrust = horSpeedConstant*Drag
    Weight = mass * grav

    acc_hor_this = sumaF_hor(Drag, Thrust, mass)
    acc_ver_this = sumaF_ver(Lift, Weight, mass)

    # xcg = 0.374
    # xcg = moveXCG(alpha_this_true)
    if(vel_vert_this < 0):
        if(alpha_this_true >= alphaStall):
            vel_hor_this = 17
            xcg = 0.390
        elif (alpha_this_true < 0):
            vel_hor_this = 16
            xcg = 0.410
```

```
        else:
            vel_hor_this = 16
            xcg = 0.405
    elif(vel_vert_this > 0):
        vel_hor_this = 15
        xcg = 0.390
    else:
        vel_hor_this = 16
        xcg = 0.400

    XCG.append(0.400)
    acc_ang_this = sumaMpitch(alpha_this_true, xcg, dynamicPressure)
    height_this = height[i-1] + vel_vert_prev*dt + 0.5 * acc_ver_prev * dt * dt

    alpha.append(alpha_this)
    alphaTrue.append(alpha_this_true)

    velHor.append(vel_hor_this)
    velVer.append(vel_vert_this)
    velAng.append(vel_ang_this)

    accHor.append(acc_hor_this)
    accVer.append(acc_ver_this)
    accAng.append(acc_ang_this)

    height.append(height_this)
    LIFT.append(Lift)
windSeries = np.array(windVerticalSpeed)

fig1 = plt.figure()
ax1 = fig1.add_subplot(1, 1, 1)
ax2 = ax1.twinx()
ax1.plot(time, height, 'r-')
ax2.plot(time, windSeries, 'b-')

ax1.grid(color='grey', linestyle='-', linewidth=0.5)
ax1.set_ylim([-10,200])
ax2.set_ylim([0,20])
ax1.set_xlim([0,600])

ax1.set_xlabel('Time [s]')
ax1.set_ylabel('Flight Altitude [m]', color='red')
```

```
ax2.set_ylabel('Wind Vertical Gust [m/s]', color='blue')

fig2 = plt.figure()
ax3 = fig2.add_subplot(1, 1, 1)
ax4 = ax3.twinx()

ax3.plot(time, alphaDeg, 'r-')
ax4.plot(time, windSeries, 'b-')

ax3.grid(color='grey', linestyle='-', linewidth=0.5)
ax3.set_ylim([-50,50])
ax4.set_ylim([0,20])
ax3.set_xlim([0,600])
ax3.set_xlabel('Time [s]')
ax3.set_ylabel('Angle of Attack [deg]', color='red')
ax4.set_ylabel('Wind Vertical Gust [m/s]', color='blue')


fig3 = plt.figure()
ax5 = fig3.add_subplot(1, 1, 1)
ax6 = ax5.twinx()


ax5.plot(time, XCG, 'r-')
ax6.plot(time, windSeries, 'b-')

ax5.grid(color='grey', linestyle='-', linewidth=0.5)
ax5.set_ylim([0.380,0.42])
ax6.set_ylim([0,20])
ax5.set_xlim([0,600])
ax5.set_xlabel('Time [s]')
ax5.set_ylabel('CoG-X position [m]', color='red')
ax6.set_ylabel('Wind Vertical Gust [m/s]', color='blue')

plt.show()
# ---------------------------------------------------------------------------
```

Part E

REFERENCES

Bibliography

[1] Nickel, K., Wohlfahrt, M. *Tailless Aircraft in Theory and Practice,* Amer Inst of Aeronautics, (September 1, 1994), AIAA Education Series, Book

[2] Guglielmo, J., Selig, M. *Spanwise Variations in Profile Drag for Airfoils at Low Reynolds Numbers,* University of Illinois at Urbana-Champaign, (July-August, 1996), Journal of Aircraft, Vol. 33, No. 4,

[3] Ira Abbott, H., Albert Von Doenhoff, E. *Theory of wing sections,* Dover Publications, Inc. New York, (1959), Dover, Book

[4] V. I. Feodosiev. *Resistencia de materiales* Mir Publishers, Moscow, (1980), Book

[5] Stephen P. Timoshenko and James M.Gere. *Theory of Elastic Stability,* Dover Publications, New York, (2009), Book

[6] E. F. Bruhn. *Analysis and Design of Flight Vehicle Structures,* Jacobs Publications, USA, (1973), Book

[7] Leishman, J. Gordon. *Principles of Helicopter Aerodynamics* Cambridge Cambridge Aerospace Series, 2000 Book

[8] Sebastián, Franchini; Óscar, López Garcia. *Introducción a la Ingeniería Aeroespacial* Madrid Editorial Garceta, 2012 Book

[9] Miguel Ángel, Gómez Tierno; Manuel, Pérez Cortés; César, Puentes Márquez. *Mecánica del vuelo* Madrid Editorial Garceta, 2012 Book

[10] European Aviation Safety Agency *EASA,* European Union 2018, Organization Official Website. Retrieved from https://www.easa.europa.eu

[11] Airfoil Tools. *Airfoil database,* 2018, Online Airfoil Database
Retrieved from http://airfoiltools.com

[12] Aerodynamics Tools. *Aerodynamics database and Tools,* 2018, Online Aerodynamics Database and Tools
Retrieved from https://www.mh-aerotools.de/airfoils/

[13] Wikipedia. *Aircraft principal axis,* 2019, Aircraft principal axis figure source
Retrieved from https://en.wikipedia.org/wiki/Aircraft_principal_axes/

[14] UIUC Airfoil Data Site. *Airfoil database,* UIUC Applied Aerodynamics Group 2018, University of Illinois at Urbana-Champaign, Dept of Aerospace Engineering
Retrieved from https://m-selig.ae.illinois.edu/

[15] Nostromo, LLC. *Nostromo-Group,* Spacir Designs 2018, Manufacturer's Official Website. Retrieved from http://nostromo-group.com/product-sets/uav-engineering-products/

[16] Ministry of Defense of Republic of Armenia. *Engineering Department,* 2018, Official Website.
Retrieved from http://www.mil.am/en

[17] Aeronautics. *Aeronautics-Systems,* AERONAUTICS 2015, Manufacturer's Official Website. Retrieved from:
https://aeronautics-sys.com/home-page/page-systems/page-systems-orbiter-2-mini-uas/

[18] C-Astral d.o.o. *C-Astral,* C-Astral 2017, Manufacturer's Official Website.
Retrieved from http://www.c-astral.com/

[19] Conyca S.L. *Conyca,* Geomax España 2018, Manufacturer's Official Website.
Retrieved from http://www.conyca.es/

[20] Primoco UAV SE. *Primoco UAV - Unmanned Aerial Vehicles and Systems,* 2018, Manufacturer's Official Website. Retrieved from http://uav-stol.com/

[21] Enics UAV JSC. *Unmanned Aerial Vehicles, Target Systems,* ACTIX studio 2018, Manufacturer's Official Website. Retrieved from http://www.enics.ru/

[22] Leonardo SPA. *Leonardo - Aerospace, Defence and Security,* Leonardo 2018, Manufacturer's Official Website. Retrieved from http://www.leonardocompany.com/en/-/falco

[23] Military Technical Institute. *Military Technical Institute, Belgrad,* 2018, Manufacturer's Official Website. Retrieved from http://www.vti.mod.gov.rs

[24] FeiyuTech. *FeiyuTech,* 2018, Manufacturer's Official Website. Retrieved from http://www.feiyu-tech.com/uav/

[25] Toray Industries, INC. *Toray,* Japan 2018, Manufacturer's Official Website.
Retrieved from https://www.toray.com/

[26] ASM Aerospace Specification Metals, Inc. *Mars Parachutes,* US 2018, Manufacturer's Official Website.
Retrieved from http://www.aerospacemetals.com/contact-aerospace-metals.html

[27] MonoKote *MonoKote* 2018, Manufacturer's Patent.
Retrieved from http://www.freepatentsonline.com/3388651.pdf and
Retrieved from http://www.monokote.com/

[28] APC Propellers *APC,* 2018, Technical Data sheet from the manufacturer's Official Website.
Retrieved from https://www.apcprop.com/files/PER3_16x10E.dat

[29] Eli Airborne Solutions *Eli Estonia,* 2019, Manufacturer's Official Website.
Retrieved from http://www.uav.ee/

[30] Hacker Motor GmbH *Hacker Motor,* 2019, Manufacturer's Official Website.
Retrieved from https://www.hacker-motor-shop.com/

[31] ArduPilot *ArduPilot Developer,* 2019, Manufacturer's Official Website.
Retrieved from http://ardupilot.org/

[32] Matek Systems *Matek Systems,* 2019, Manufacturer's Official Website.
Retrieved from http://www.mateksys.com/

[33] FlySky RC *FlySky Systems,* 2019, Manufacturer's Official Website.
Retrieved from http://www.flyskyrc.com/

[34] Advanced Microwave Products *Advanced Microwave Products* 2019, Manufacturer's Official Website.
Retrieved from https://www.advmw.com/

[35] Sony Corporation *Sony* 2019, Manufacturer's Official Website.
Retrieved from https://www.sony.com/

[36] Panasonic *Panasonic* 2019, Manufacturer's Official Website.
Retrieved from https://www.panasonic.com

[37] Hitachi Ltd. *Hitachi* 2019, Manufacturer's Official Website.
Retrieved from https://www.hitachi.com/

[38] Flir Systems Inc. *Flir* 2019, Manufacturer's Official Website.
Retrieved from https://www.flir.com/

[39] Leonardo DRS Inc. *Leonardo DRS* 2019, Manufacturer's Official Website. Retrieved from http://www.drsinfrared.com/Home.aspx

[40] North American Survival Systems *NA Survival Systems* 2019, Manufacturer's Official Website. Retrieved from https://northamericansurvivalsystems.com

[41] L3 Technologies Inc. *L3 Warrior Sensor Systems* 2019, Manufacturer's Official Website. Retrieved from http://www.l3warriorsystems.com/ nanocore